Synthesis of the Bifunctional Phosphinidene Cluster, $Fe_3(CO)_9(\mu_3\text{-}PH)_2$, and a Systematic Study of the Reactivity of the Cluster-Bound P−H Functional Group

Caryn C. Borg-Breen, Maria T. Bautista, Cynthia K. Schauer,* and Peter S. White

Contribution from the Department of Chemistry, The University of North Carolina at Chapel Hill, Chapel Hill, North Carolina 27599-3290

Received October 26, 1999

Abstract: The synthesis and systematic study of the reaction chemistry of a bifunctional phosphinidene cluster, $Fe_3(CO)_9(\mu_3\text{-}PH)_2$ (**3**) is reported. Reaction chemistry at one P−H functional site is effectively communicated through the $Fe_3(CO)_9$ core, and impacts on the reactivity of the second P−H site. Deprotonation of the acidic protons in **3** allows access to a lone electron pair on phosphorus. The first proton is readily removed with NEt_3/[PPN]Cl ($[PPN]^+ = (Ph_3P)_2N^+$) to produce the $[PPN]^+$ salt of $[Fe_3(CO)_9(\mu_3\text{-}PH)(\mu_3\text{-}P)]^-$ ([**4**]$^-$). Removal of both phosphorus-bound hydrogen atoms in **3** requires the use of 2 equiv of *n*-BuLi, to produce $Li_2[Fe_3(CO)_9(\mu_3\text{-}P)_2]$ (Li_2[**5**]). Quenching of Li_2[**5**] with MeOH-d_4 generates $[Fe_3(CO)_9(\mu_3\text{-}PD)(\mu_3\text{-}P)]^-$. The lone electron pairs on the cluster-bound phosphorus atoms undergo analogous reaction chemistry to organophosphines. Alkylation at the phosphorus site is carried out by reaction of [Et_3NH][**4**] with $MeOSO_2CF_3$ generating the monosubstituted cluster, $Fe_3(CO)_9(\mu_3\text{-}PMe)(\mu_3\text{-}PH)$ (**6**) as the primary product. The cluster anions [**4**]$^-$ and [**8**]$^-$, containing a phosphorus lone pair, are oxidized by elemental sulfur to produce the phosphine sulfide complexes, [Et_3NH][$Fe_3(CO)_9(\mu_3\text{-}PH)(\mu_3\text{-}P{=}S)$] ([$Et_3NH$][**10**]) and [$Et_3NH$][$Fe_3(CO)_9(\mu_3\text{-}PMe)(\mu_3\text{-}P{=}S)$] ([$Et_3NH$][**11**]). Treatment of [**10**]$^-$ with an additional equivalent of NEt_3 and S_8 yields the dianionic cluster, $[Et_3NH]_2[Fe_3(CO)_9(\mu_3\text{-}P{=}S)_2]$ ($[Et_3NH]_2$[**12**]). Without added base, reaction of the neutral clusters, **3** and **6**, with S_8 in THF solution yield the clusters $Fe_3(CO)_9(\mu_3\text{-}PH)(\mu_3\text{-}PSCH_2CH_2CH_2CH_2OH)$ (**13**), $Fe_3(CO)_9(\mu_3\text{-}PSCH_2CH_2CH_2CH_2OH)_2$ (**14**), and $Fe_3(CO)_9(\mu_3\text{-}PMe)(\mu_3\text{-}PSCH_2CH_2CH_2CH_2OH)$ (**15**), with a ring-opened THF molecule appended to sulfur. Reaction of **3** with S_8 in THF solution in the presence of $ClAuPPh_3$ produces the gold derivative, $Fe_3(CO)_9(\mu_3\text{-}PSAuPPh_3)_2$ (**17**). Like PH groups in phosphines, the μ_3-PH moieties in **3** react with activated alkenes to yield single- and double-insertion products, $Fe_3(CO)_9(\mu_3\text{-}PH)(\mu_3\text{-}PCH_2CH_2R)$ (R = CN (**18a**), CO_2Me (**19a**)) and $Fe_3(CO)_9(\mu_3\text{-}PCH_2CH_2R)_2$ (R = CN (**18b**), CO_2Me (**19b**)). The solid-state structures of **3**, **17**, and **18b** were determined by single-crystal X-ray diffraction.

Introduction

Tertiary organophosphine ligands (R_3P, R = alkyl, aryl) have played a vital role in the development of organometallic chemistry and homogeneous catalysis.[1] The donor ability and steric properties of the phosphine ligand can be widely varied by the choice of the substituents on the phosphorus atom. Analogous to organophosphine ligands, transition metal clusters with a phosphorus atom adopting a face-bridging position have a lone electron pair that is capable of acting as a ligand (e.g., see **I**, Scheme 1). There are relatively few examples of clusters of type **I**,[2] due to the high reactivity of the phosphorus site under the conditions for cluster synthesis. To systematically access chemistry at cluster-bound phosphorus atoms, we have developed syntheses for silylphosphinidene clusters (**II**).[3] The bulky silyl substituents act as a protecting group for the phosphorus ligand during the cluster synthesis and can then be cleaved by a variety of reagents to access the phosphorus site for reactions.[4,5] The product of hydrolysis of a silylphosphinidene cluster is a μ_3-PH-capped cluster complex, **III**.[6] Clusters with P−H

Scheme 1

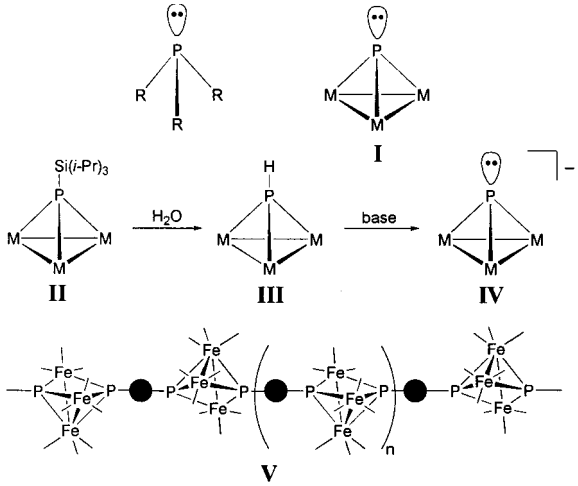

(1) Levason, W. In *The Chemistry of Organophosphorus Compounds*; Hartley, F. R., Ed.; John Wiley and Sons: New York, 1990; Vol. 1, Chapter 15, and references therein.

(2) (a) Scherer, O. J. *Angew. Chem., Int. Ed. Engl.* **1990**, *29*, 1104−1122. (b) Scherer, O. J.; Weigel, S.; Wolmershäuser, G. *Chem. Eur. J.* **1998**, *4*, 1910−1916. (c) Davies, J. E.; Klunduk, M. C.; Mays, M. J.; Raithby, P. R.; Shields, G. P.; Tompkin, P. K. *J. Chem. Soc., Dalton Trans.* **1997**, 715. (d) Foerstner, J.; Olbrich, F.; Butenschön, H. *Angew. Chem., Int. Ed. Engl.* **1996**, *35*, 1234−1237. (e) Kilthau, T.; Nuber, B.; Ziegler, M. L. *Chem. Ber.* **1995**, *128*, 197−199.

(3) (a) Sunick, D. L.; White, P. S.; Schauer, C. K. *Organometallics* **1993**, *12*, 245−247. (b) Bautista, M. T.; White, P. S.; Schauer, C. K. *J. Am. Chem. Soc.* **1991**, *113*, 8963−8965. (c) Bautista, M. T.; Jordan, M. R.; White, P. S.; Schauer, C. K. *Inorg. Chem.* **1993**, *32*, 5429−5430.

10.1021/ja993811f CCC: $19.00
Published on Web 04/08/2000

bonds are readily deprotonated to produce anionic cluster-based phosphine ligands (**IV**).

An understanding of the reactivity of the cluster-based phosphine ligands is an important goal in our program to assemble extended structures, taking advantage of reactions at cluster-bound phosphorus atoms.[7] A *bifunctional* cluster, $[Fe_3(CO)_9(\mu_3\text{-}P)_2]^{2-}$, in which there are two reactive phosphorus sites, is ideally suited for the preparation of a one-dimensional, *linear* cluster chain (**V**). Because the $Fe_3(CO)_9$ core effectively mediates communication between the two phosphorus sites, stepwise reaction chemistry to assemble chains is possible. We report herein the synthesis of the bicapped silylphosphinidene cluster, $Fe_3(CO)_9[\mu_3\text{-}PSi(i\text{-}Pr)_3]_2$ (**2**), hydrolysis of **2** to prepare $Fe_3(CO)_9(\mu_3\text{-}PH)_2$ (**3**),[3c] deprotonation reactions of **3** to generate cluster-based phosphine ligands, and a systematic study of organophosphine-like reactions of the cluster functional group, including alkylation, oxidation, and alkene insertion. Remarkably, the same spectrum of reaction chemistry observed for organophosphines is also possible with the cluster-bound functional group.

Results and Discussion

Synthesis of $Fe_3(CO)_9(\mu_3\text{-}PR)_2$ (R = SiR_3, H). Several bicapped triiron phosphinidene cluster complexes, $Fe_3(CO)_9(\mu_3\text{-}PR)_2$, have been prepared from iron pentacarbonyl and primary phosphines, H_2PR.[8,9] Cluster complexes containing a silylphosphinidene ligand can be prepared using a primary silylphosphine H_2PSiR_3 as a reagent.[10] Yields of the product silylphosphinidene clusters are higher with bulkier silylphosphine reagents such as $H_2PSi(i\text{-}Pr)_3$. Heating a toluene solution of $Fe_3(CO)_{12}$ with 1 equiv of $H_2PSi(i\text{-}Pr)_3$ at 60 °C yields a single phosphorus-containing product in the $^{31}P\{^1H\}$ NMR which is identified as the monocapped phosphinidene cluster, $Fe_3(CO)_9(\mu\text{-}CO)[\mu_3\text{-}PSi(i\text{-}Pr)_3]$, on the basis of the NMR and IR data[11] (Scheme 2). Continued heating at 60 °C following addition of a second equiv of $H_2PSi(i\text{-}Pr)_3$ produces a new

Scheme 2

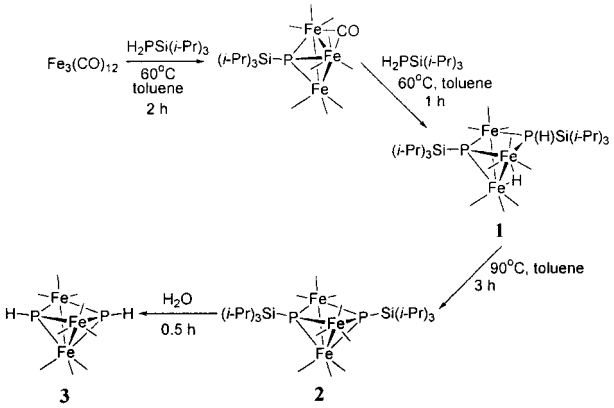

species as the primary product characterized by doublets at δ 255 and −239 (^2J(P,P) = 124) in the $^{31}P\{^1H\}$ NMR spectrum. This product is assigned as the phosphinidene/phosphido cluster, $(\mu\text{-}H)Fe_3(CO)_9[\mu\text{-}P(H)Si(i\text{-}Pr)_3][\mu_3\text{-}PSi(i\text{-}Pr)_3]$ (**1**) based on its similarity to structurally characterized analogues.[12] Addition of the silylphosphine in two separate steps results in a higher yield of phosphinidene products than a one-step addition of all of the phosphine. Conversion of **1** to the bicapped phosphinidene cluster, $Fe_3(CO)_9[\mu_3\text{-}PSi(i\text{-}Pr)_3]_2$ (**2**), is achieved by heating the solution at 90 °C. Attempts to purify **2** by column chromatography were unsuccessful due to reactions with column supports, even at −40 °C.

The silylphosphinidene cluster, **2**, serves as a precursor to the parent phosphinidene cluster. The reaction of **2** with excess H_2O in toluene solution cleanly produces $Fe_3(CO)_9(\mu_3\text{-}PH)_2$ (**3**) as the major P−H capped cluster product. Purification of **3** by column chromatography, followed by crystallization of the residue from cold hexanes produces a red-purple solid that is isolated in 30% yield (based on the starting silylphosphine). The two sets of symmetry equivalent but magnetically inequivalent NMR active nuclei in cluster **3** constitute an AA′XX′ spin system characterized by two chemical shifts (δ_A, $\mu_3\text{-}PH_A$, and δ_X, $\mu_3\text{-}P_XH$) and four coupling constants ($J_{AA'}$, $J_{XX'}$, J_{AX}, $J_{AX'}$). The AA′ multiplet is observed at δ 4.07 in the ^1H NMR (Figure 1) near the values observed for other P−H capped clusters such as $CrCo_2(CO)_{11}(\mu_3\text{-}PH)$ (δ 4.15)[6a] and $FeCo_2(CO)_9(\mu_3\text{-}PH)$ (δ 4.67).[6d] An identical XX′ multiplet is observed in the ^{31}P NMR spectrum at δ 235.1 (see Table 1). Using standard analysis of AA′XX′ patterns, the coupling constants of ^1J(H,P) = ± 316, ^3J(H,P) = ± 14, ^4J(H,H) = ± 9 and ^2J(P,P) = ± 338 are obtained.[13] The structure of **3** was determined by a single-crystal X-ray diffraction study. A thermal ellipsoid plot for **3** is shown in Figure 2 and crystal data are given in Table 3. The Fe_3-triangle is characterized by two Fe−Fe bonds ($Fe\text{-}Fe_{avg}$ = 2.720 (10) Å)[14] and a nonbonding interaction (Fe···Fe = 3.561 (2) Å). The two unique Fe−P bond types have very similar bond lengths ($Fe_{apical}\text{-}P_{avg}$ = 2.224 (4) Å, $Fe_{basal}\text{-}P_{avg}$ = 2.213 (10)

(4) Reactions of silylphosphines $(SiMe_3)_2PR$ and $(SiMe_3)PR_2$ have been utilized to prepare phosphido-bridged complexes and phosphinidene-capped clusters. See, for example: (a) Fenske, D.; Ohmer, J.; Hachgenei, J.; Merzweiler, K. *Angew Chem., Int. Ed. Engl.* **1988**, *27*, 1277−1296. (b) Schäfer, H.; Zipfel, J.; Gutekunst, B.; Lemmert, U.; *Z. Anorg. Allg. Chem.* **1985**, *529*, 157.

(5) Methanolysis of $P(SiMe_3)_2$-bridged complexes have been utilized to prepare 12/15 semiconductor particles. (a) Goel, S. C.; Chiang, M. Y.; Buhro, W. E. *J. Am. Chem. Soc.* **1990**, *112*, 5636−5637. (b) Matchett, M. A.; Viano, A. M.; Adolphi, N. L.; Stoddard, R. D.; Buhro, W. E.; Conradi. M. S.; Gibbons, P. C. *Chem. Mater.* **1992**, *4*, 508−511.

(6) For examples of monocapped μ_3-PH or μ_4-PH clusters, see: (a) Austin, R. G.; Urry, G. *Inorg. Chem.* **1977**, *16*, 3359−3360. (b) Ebsworth, E. A. V.; McIntosh, A. P.; Schröder, M. *J. Organomet. Chem.* **1986**, *312*, C41−C43. (c) Brauer, D. J.; Hasselkuss, G.; Hietkamp, S.; Sommer, H.; Stelzer, O. *Z. Naturforsch.* **1985**, *40b*, 961−967. (d) Honrath, U.; Liu, S.-T.; Vahrenkamp, H. *Chem. Ber.* **1985**, *118*, 132−143. (e) Heuer, L.; Nordlander, E.; Johnson, B. F. G.; Lewis, J.; Raithby, P. R. *Phosphorus, Sulfur, Silicon* **1995**, *103*, 241−252. (f) Johnson, B. F. G.; Lewis, J.; Nordlander, E.; Raithby, P. R. *J. Chem. Soc., Dalton Trans.* **1996**, 755−763. (g) Colbran, S. B.; Lahoz, F. L.; Raithby, P. R.; Lewis, J.; Johnson, B. F. G.; Cardin, C. *J. Chem. Soc., Dalton Trans.* **1988**, 173−181.

(7) (a) Bautista, M. T.; White, P. S.; Schauer, C. K. *J. Am. Chem. Soc.* **1994**, *116*, 2143−2144. (b) Jordan, M. R.; White, P. S.; Schauer, C. K.; Mosley, M. A. *J. Am. Chem. Soc.* **1995**, *117*, 5403−5404. (c) Bautista, M. T.; White, P. S.; Schauer, C. K., manuscript in preparation. (d) Borg-Breen, C. C.; Schauer, C. K.; White, P. S., manuscript in preparation.

(8) Treichel, P. M.; Dean, W. K.; Douglas, W. M. *Inorg. Chem.* **1972**, *11*, 1609−1615.

(9) Bartsch, R.; Hietkamp, S.; Morton, S.; Stelzer, O. *J. Organomet. Chem.* **1981**, *222*, 263.

(10) We have previously reported a synthesis of the bifunctional cluster complex, $(\mu\text{-}H)Fe_3(CO)_9[\mu\text{-}P(H)(SiMe_3)](\mu_3\text{-}PSiMe_3)$, from a low-temperature reaction between $Fe(CO)_3(coe)_2$ (coe = *cis*-cyclooctene) and H_2PSiMe_3. However isolation of this product using standard methods was not possible. See ref 3(b).

(11) $Fe_3(CO)_9(\mu\text{-}CO)[\mu_3\text{-}PSi(i\text{-}Pr)_3]$: $^{31}P\{^1H\}$ NMR (δ, ppm, toluene) 378 (s); IR (ν_{CO}, cm^{-1}, toluene) 2078 (w), 2050 (m), 2038 (s), 2020 (vs), 1994 (m), 1968 (vw), 1851 (vw). Compare with $Fe_3(CO)_9(\mu\text{-}CO)(\mu_3\text{-}PPh)$: IR ($\nu_{CO}$, cm^{-1}, pentane) 2084 (w) 2042 (s), 2030 (vs), 2015 (m), 1992 (vw), 1983 (vw), 1969 (vw), 1859 (vw) in Lang, H.; Zsolnai, L.; Huttner, G. *J. Organomet. Chem.* **1985**, *282*, 23−51.

(12) Brauer, D. J.; Hietkamp, S.; Sommer, H.; Stelzer, O.; Müller, G.; Krüger, C. *J. Organomet. Chem.* **1985**, *288*, 35−61.

(13) See, for example, any text dealing with high-resolution NMR: Becker, E. D. *High-Resolution NMR: Theory and Chemical Applications*; Academic Press: New York, 1969; pp 166−170.

(14) A root-mean-square estimated standard deviation is reported for all average distances.

Table 1. ^{31}P (δ, ppm) Data[a]

compound	μ_3-P_A	μ_3-P_B	J (Hz)
	neutrals		
$Fe_3(CO)_9(\mu_3\text{-}PH)_2$ (**3**)	235 XX′, *P*H[b]		$^2J(P,P) = 338$, $^1J(H,P) = 316$, $^3J(H,P) = 14$
$Fe_3(CO)_9(\mu_3\text{-}PH)(\mu_3\text{-}PMe)$ (**6**)	231 dd, *P*H[e]	327 dqt, *P*Me	$^2J(P,P) = 323$, $^1J(H,P) = 315$, $^2J(H,P) = 13$
$Fe_3(CO)_9(\mu_3\text{-}PMe)_2$ (**7**)	320 v st, *P*Me[h]		$\lvert^2J(H,P) + {}^4J(H,P)\rvert = 15$
$Fe_3(CO)_9(\mu_3\text{-}PEt)_2$	343 s, *P*Et[h]		
$Fe_3(CO)_9(\mu_3\text{-}PH)(\mu_3\text{-}PS(CH_2)_4OH)$ (**13**)	230 d, *P*H[g]	361 d, *P*SCH_{2-}	$^2J(P,P) = 280$, $^1J(P,H) = 312$
$Fe_3(CO)_9(\mu_3\text{-}PS(CH_2)_4OH)_2$ (**14**)	359 s, *P*SCH_{2-}[c]		$^3J(P,H) = 6.1$, $^2J(P,C) = 10$
$Fe_3(CO)_9(\mu_3\text{-}PMe)(\mu_3\text{-}PS(CH_2)_4OH)$ (**15**)	318 d, *P*Me[c]	360 d, *P*SCH_{2-}	$^2J(P,P) = 259$, $^2J(P,H) = 12.6$, $^3J(P,H) = 6$
$Fe_3(CO)_9(\mu_3\text{-}PSAuPPh_3)_2$ (**17**)	388 s, *P*SAuPPh$_3$c		
$Fe_3(CO)_9(\mu_3\text{-}PH)(\mu_3\text{-}P(CH_2)_2CN)$ (**18a**)	235 d, *P*H[g]	321 d, *P*CH_{2-}	$^2J(P,P) = 315$
$Fe_3(CO)_9(\mu_3\text{-}P(CH_2)_2CN)_2$ (**18b**)	321 s, *P*CH_{2-}[g]		
$Fe_3(CO)_9(\mu_3\text{-}PH)(\mu_3\text{-}P(CH_2)_2CO_2Me)$ (**19a**)	235 d, *P*H[g]	337 d, *P*CH_{2-}	$^2J(P,P) = 313$
$Fe_3(CO)_9(\mu_3\text{-}P(CH_2)_2CO_2Me)_2$ (**19b**)	335 s, *P*CH_{2-}[g]		
	monoanions[i]		
$[HNEt_3][Fe_3(CO)_9(\mu_3\text{-}PH)(\mu_3\text{-}P)]$ ([$HNEt_3$][**4**])	286 dd, *P*H[d]	431 d, P	$^2J(P,P) = 35$, $^1J(H,P) = 241$
$[PPN][Fe_3(CO)_9(\mu_3\text{-}PH)(\mu_3\text{-}P)]$ ([PPN][**4**])	278 dd, *P*H[c]	535 dd, P	$^2J(P,P) = 35$, $^1J(H,P) = 211$, $^3J(H,P) = 11$
$Li[Fe_3(CO)_9(\mu_3\text{-}PD)(\mu_3\text{-}P)]$	278 dt, *P*D[g]	532 d, P	$^2J(P,P) = 34$, $^1J(D,P) = 34$
$[HNEt_3][Fe_3(CO)_9(\mu_3\text{-}PMe)(\mu_3\text{-}P)]$ ([$HNEt_3$][**8**])	363 br s, *P*Me[h]	410 br s, P	$^2J(P,P) = 30$
[PPN][$Fe_3(CO)_9(\mu_3\text{-}PMe)(\mu_3\text{-}P)$] ([PPN][**8**])	357 dqt, *P*Me[g]	513 d, P	$^2J(P,P) = 35$, $^2J(H,P) = 11$
$[HNEt_3][Fe_3(CO)_9(\mu_3\text{-}PH)(\mu_3\text{-}P{=}S)]$ ([$HNEt_3$][**10**])	231 dd, *P*H[g]	409 dd, *P*=S	$^2J(P,P) = 257$, $^1J(H,P) = 291$, $^3J(P,H) = 20$
$[HNEt_3][Fe_3(CO)_9(\mu_3\text{-}PMe)(\mu_3\text{-}P{=}S)]$ ([$HNEt_3$][**11**])	321 d, *P*Me[g]	406 d, *P*=S	$^2J(P,P) = 240$, $^2J(H,P) = 10$
$[HNEt_3][Fe_3(CO)_9(\mu_3\text{-}PS(CH_2)_4OH)(\mu_3\text{-}P{=}S)]$ ([**16**]$^-$)	365 d, *P*SCH_{2-}[c]	401 d, *P*=S	$^2J(P,P) = 197$
	dianions[i]		
$Li_2[Fe_3(CO)_9(\mu_3\text{-}P)_2]$ (Li_2[**5**])	616 s, *P*[g]		
$[HNEt_3]_2[Fe_3(CO)_9(\mu_3\text{-}P{=}S)_2]$ ([$HNEt_3$]$_2$[**12**])	412 s, *P*=S[g]		
$Li_2[Fe_3(CO)_9(\mu_3\text{-}P{=}S)_2]$ (Li_2[**12**])	420 s, *P*=S[g]		

[a] s = singlet, d = doublet, dd = doublet of doublets, t = triplet, qt = quartet, pt = pentet, st = septet, m = multiplet, br = broad, v = virtual. [b] toluene-d_8. [c] THF-d_8. [d] CD_2Cl_2. [e] C_6D_6. [f] $CDCl_3$. [g] THF. [h] CH_2Cl_2. [i] At −80 °C.

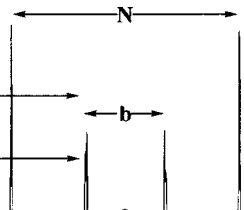

3

Figure 1. ^{1}H NMR spectrum of $Fe_3(CO)_9(\mu_3\text{-}PH)_2$ (**3**) in toluene-d_8.

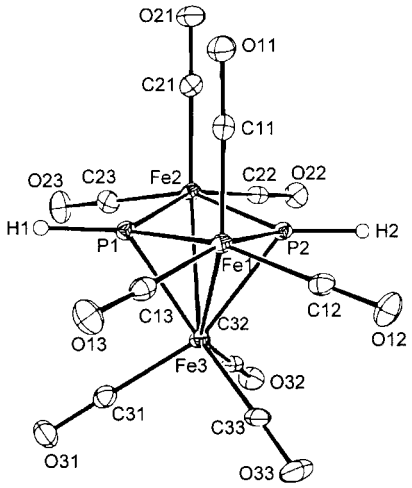

Figure 2. Diagram of $Fe_3(CO)_9(\mu_3\text{-}PH)_2$ (**3**), showing the thermal ellipsoids (50% probability level) and the atomic labeling scheme.

Å). The short nonbonding distance between the two phosphorus nuclei of 2.582(2) Å enforced by the open triangle is only ∼0.3 Å longer than a P−P single bond (∼2.22 Å) in organophosphorus compounds.[15] The structural parameters of **3** do not differ significantly from those for the phenylphosphinidene cluster complex, $Fe_3(CO)_9(\mu_3\text{-}PPh)_2$.[16]

Deprotonation of $Fe_3(CO)_9(\mu_3\text{-}PH)_2$. While phosphinidene ligands are usually considered to be four-electron donors, the μ_3-PH ligands in $Fe_3(CO)_9(\mu_3\text{-}PH)_2$ may also be viewed as cluster-based phosphonium ions, where a −2 charge resides on the cluster and the μ_3-PH groups act as three-electron donors to the 50-electron cluster (eq 1). The assignment as a phosphonium ion is consistent with the high acidity of the first phosphorus-bound hydrogen atoms in **3**, which is readily removed as H^+ by reaction with NEt_3/[PPN]Cl ([PPN]$^+$ = $(Ph_3P)_2N^+$) to produce the [PPN]$^+$ salt of red-orange $[Fe_3(CO)_9(\mu_3\text{-}PH)(\mu_3\text{-}P)]^-$ ([**4**]$^-$).[17] The CO stretching pattern observed in the infrared spectrum of [PPN][**4**] is nearly identical to that observed for **3**, but is shifted by 50 cm^{-1} to lower energy (see

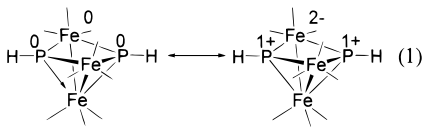

(1)

(15) Gilheany, D. G. In *The Chemistry of Organophosphorus Compounds*; F. R. Hartley, Ed.; Wiley: New York, 1990; Vol. 1; pp Chapter 2.

(16) Cook, S. L.; Evans, J.; Gray, L. R.; Webster, M. *J. Organomet. Chem.* **1982**, *236*, 367−374.

(17) Assignment of a 2− charge to the cluster core is also consistent with our observation of two-electron $Fe_3(CO)_9$ core-based redox chemistry for clusters in which the phosphinidene is bound to transition metal capping group fragments, ML_n (see: Koide, Y.; Bautista, M. T.; White, P. S.; Schauer, C. K. *Inorg. Chem.* **1992**, *31*, 3690−3692).

Table 2. IR Data

compound	ν_{CO} (cm^{-1})[a]
	neutrals
$Fe_3(CO)_9(\mu_3\text{-}PH)_2$ (**3**)[b]	**2051 (vs)**, 2031 (vs), 2014 (s), 2006 (w), 1997 (w), 1977 (vw)
$Fe_3(CO)_9(\mu_3\text{-}PMe)(\mu_3\text{-}PH)$ (**6**)[b]	**2047 (vs)**, 2026 (vs), 2008 (s), 1999 (w), 1990 (w), 1971 (vw)
$Fe_3(CO)_9(\mu_3\text{-}PMe)_2$ (**7**)[b]	**2040 (vs)**, 2021 (vs), 2002 (s)
$Fe_3(CO)_9(\mu_3\text{-}PS(CH_2)_4OH)_2$ (**14**)[d]	2075 (w), **2044 (vs)**, 2020 (s), 2008 (m), 1993 (m)
$Fe_3(CO)_9(\mu_3\text{-}PMe)(\mu_3\text{-}PS(CH_2)_4OH)$ (**15**)[d]	**2041 (vs)**, 2018 (s), 2004 (m), 1993 (m)
$Fe_3(CO)_9(\mu_3\text{-}PSAuPPh_3)_2$ (**17**)[d]	**2026 (vs)**, 2003 (s), 1990 (m), 1975 (m)
$Fe_3(CO)_9(\mu_3\text{-}PEt)_2$[c]	**2038 (vs)**, 2016 (s), 1997 (m)
$Fe_3(CO)_9(\mu_3\text{-}P(CH_2)_2CN)_2$ (**18b**)[c]	2078 (vw), **2045 (vs)**, 2024 (vs), 2003 (m), 2256 (vw, CN)
$Fe_3(CO)_9(\mu_3\text{-}P(CH_2)_2CO_2Me)_2$ (**19b**)[c]	2073 (vw), **2041 (vs)**, 2018 (vs), 1998 (m), 1738 (w, C═O(OMe))
	monoanions[e]
$[HNEt_3][Fe_3(CO)_9(\mu_3\text{-}PH)(\mu_3\text{-}P)]$ ($[HNEt_3][\mathbf{4}]$)[c]	2049 (m), 2026 (m), **2012 (vs)**, 1992 (s), 1965 (br m)
$[PPN][Fe_3(CO)_9(\mu_3\text{-}PH)(\mu_3\text{-}P)]$ ($[PPN][\mathbf{4}]$)[d]	2040 (vw), 2024 (vw), **2002 (vs)**, 1980 (s), 1956 (m), 1944 (sh)
$[HNEt_3][Fe_3(CO)_9(\mu_3\text{-}PMe)(\mu_3\text{-}P)]$ ($[HNEt_3][\mathbf{8}]$)[c]	2045 (w), 2022 (w), **2007 (vs)**, 1987 (s), 1959 (br m)
$[PPN][Fe_3(CO)_9(\mu_3\text{-}PMe)(\mu_3\text{-}P)]$ ($[PPN][\mathbf{8}]$)[d]	2037 (vw), 2019 (vw), **1997 (vs)**, 1976 (vs), 1951 (s), 1939 (sh)
$[HNEt_3][Fe_3(CO)_9(\mu_3\text{-}PH)(\mu_3\text{-}P{=}S)]$ ($[HNEt_3][\mathbf{10}]$)[d]	2036 (w), **2018 (vs)**, 1997 (s), 1977 (m)
$[HNEt_3][Fe_3(CO)_9(\mu_3\text{-}PMe)(\mu_3\text{-}P{=}S)]$ ($[HNEt_3][\mathbf{11}]$)[d]	2033 (w), **2013 (vs)**, 1992 (s), 1972 (m)
$[HNEt_3][Fe_3(CO)_9(\mu_3\text{-}PS(CH_2)_4OH)(\mu_3\text{-}P{=}S)]$ ($[HNEt_3][\mathbf{16}]$)[d]	2038 (w), **2017 (vs)**, 1995 (s), 1976 (s)
	dianions[e]
$[Li]_2[Fe_3(CO)_9(\mu_3\text{-}P)_2]$ ($[Li]_2[\mathbf{5}]$)[d]	**1956 (vs)**, 1940 (s), 1930 (m), 1911 (m)
$[HNEt_3]_2[Fe_3(CO)_9(\mu_3\text{-}P{=}S)_2]$ ($[HNEt_3]_2[\mathbf{12}]$)[d]	2038 (vw), 2026 (vw), **2002 (vs)**, 1978 (s), 1962 (m), 1944 (sh)
$[Li]_2[Fe_3(CO)_9(\mu_3\text{-}P{=}S)_2]$ ($Li_2[\mathbf{12}]$)[d]	**1994 (vs)**, 1972 (s), 1955 (m), 1937 (sh)

[a] vw = very weak, w = weak, m = medium, s = strong, vs = very strong, sh = shoulder, br= broad. [b] Hexanes. [c] CH_2Cl_2. [d] THF. [e] −80 °C.

Table 3. Comparison of Crystal Parameters and Structural Features for $Fe_3(CO)_9(\mu_3\text{-}PR)_2$ Cluster Compounds

compound	$Fe_3(CO)_9(\mu_3\text{-}PH)_2$ (**3**)	$Fe_3(CO)_9(\mu_3\text{-}PSAuPPh_3)_2$ (**17**)	$Fe_3(CO)_9(\mu_3\text{-}PCH_2CH_2CN)_2$ (**18b**)
formula	$C_9H_2Fe_3O_9P_2$	$C_{45}H_{30}Au_2Fe_3O_9P_4S_2$	$C_{15}H_8Fe_3N_2O_9P_2$
fw (amu)	483.60	1464.20	589.72
crystal system	triclinic	monoclinic	monoclinic
space group	$P\bar{1}$	Cc	$P2_1/c$
color	red-brown	red-orange	red-orange
a (Å)	9.159 (6)	16.8779 (7)	11.7382 (5)
b (Å)	12.792 (4)	14.4419 (6)	9.7384 (4)
c (Å)	6.975 (2)	21.1256 (9)	18.6132 (8)
β (deg)	112.03 (3)	107.633 (1)	99.906 (1)
volume ($Å^3$)	751.5 (6)	4907.4 (4)	2095.9 (2)
temp (°C)	25	−100	25
Z	2	4	4
R	0.036	0.022	0.023
GOF	1.66	1.36	2.66
diffractometer	Rigaku AFC6S	Siemens SMART	Siemens SMART
Fe(1)−Fe(2)	2.727 (2)	2.713 (1)	2.7178 (3)
Fe(2)−Fe(3)	2.713 (1)	2.686 (1)	2.7097 (3)
Fe(1)−Fe(3)	3.561 (2)	3.560 (1)	3.5671 (3)
P(1)···P(2)	2.582 (2)	2.613 (2)	2.5775 (5)
$(Fe_{apical}-P)_{avg}$	2.224 (4)	2.218 (2)	2.2125 (4)
$(Fe_{basal}-P)_{avg}$	2.213 (1)	2.240 (1)	2.2394 (4)
$(P-R)_{avg}$	1.365 (R = H)	2.059 (2) (R = $SAuPPh_3$)	1.840 (1) (R = CH_2CH_2CN)
Fe(1)−Fe(2)−Fe(3)	49.28 (4)	48.42 (2)	49.010 (6)
Fe(1)−Fe(3)−Fe(2)	81.78 (5)	82.51 (3)	82.176 (8)
Fe(2)−Fe(1)−Fe(3)	48.94 (4)	49.07 (2)	48.814 (6)
$(P-P-R)_{avg}$	178.65 (R = H)	178.59 (9) (R = $SAuPPh_3$)	175.91 (7) (R = CH_2CH_2CN)

Table 2, Figure 3a). The ^{31}P resonance for the deprotonated phosphorus atom at δ 535.1 (THF-d_8) in [PPN][**4**] is sharp and downfield from the resonance for the P−H phosphinidene at δ 277.5 (see Table 1). A downfield shift of the ^{31}P resonance is similarly observed upon replacement of a phosphorus-bound hydrogen atom in primary or secondary organophosphines by lithium.[18] The removal of a proton from **3** has a pronounced effect on the coupling constants in the ^{31}P NMR. The $^2J(P,P)$ value for [PPN][**4**] of 35 Hz is reduced by nearly an order of magnitude from the $^2J(P,P)$ value of 338 Hz for **3**. Furthermore, there is a large change in the $^1J(H,P)$ value (from 316 in **3** to 211 in [PPN][**4**], see Table 1). The lone pair on phosphorus in [PPN][**4**] prefers to be in an orbital with a high percentage of s character.[19] The observed changes in coupling likely result from changes in the character of the orbitals involved in cluster bonding as a result of this preference.

When NEt_3 is employed as a base to deprotonate **3** in the absence of [PPN]Cl, the spectroscopic parameters for [Et_3NH][**4**] are dependent on the solvent. In THF solution, the CO stretching frequencies of [Et_3NH][**4**] are nearly identical to those of [PPN][**4**], while in CH_2Cl_2 solution, the strongest intensity

(18) (a) Zschunke, A.; Bauer, E.; Schmidt, H.; Issleib, K. *Z. Anorg. Allg. Chem.* **1982**, *495*, 115−119. (b) Bartlett, R. A.; Olmstead, M. M.; Power, P. P.; Siegel, G. A. *Inorg. Chem.* **1987**, *26*, 1941−1946.

(19) Increased s character of the phosphorus orbital is also suggested to account for the small Fe−E−Fe bond angles (96°−97°) observed for $[Fe_3(CO)_9(\mu_3\text{-}E)_2]^{2-}$ (E = Se, Te) and $Fe_3(CO)_9(\mu_3\text{-}E)_2$ (E = As, Bi) clusters. See: (a) Bachman; R. E.; Miller, S. K.; Whitmire, K. H. *Organometallics* **1995**, *14*, 796−803. (b) Eveland, J. R.; Saillard, J.-Y.; Whitmire, K. H. *Inorg. Chem.* **1997**, *36*, 330−334. (c) Collins, B. E.; Koide, Y.; Schauer, C. K.; White, P. S. *Inorg. Chem.* **1997**, *36*, 6172−6183.

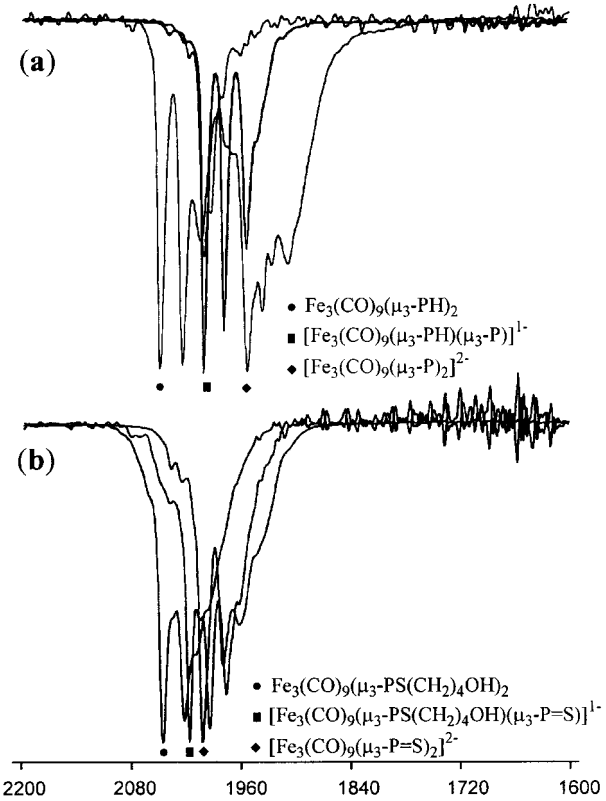

Figure 3. Infrared spectra in THF (ν_{CO}) for (a) **3**, $[HNEt_3][\mathbf{4}]$, and $[HNEt_3]_2[\mathbf{5}]$; (b) **13**, $[HNEt_3][\mathbf{16}]$, and $[HNEt_3]_2[\mathbf{12}]$.

Scheme 3

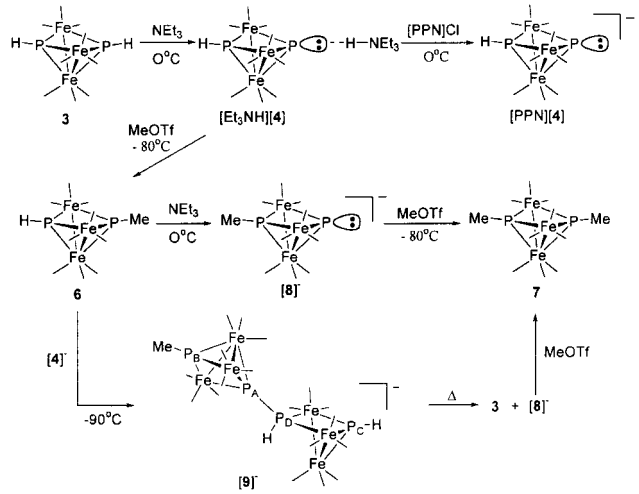

carbonyl stretch occurs at 2012 cm^{-1}, intermediate between that of **3** (2051 cm^{-1}) and [PPN][**4**] (2002 cm^{-1}) in THF solution (see Table 2). This intermediate energy shift suggests that the lone pair on phosphorus is acting as a hydrogen bond acceptor from the $[Et_3NH]^+$ counterion (see Scheme 3). Since the strong intensity CO stretch for $[Et_3NH][\mathbf{4}]$ is shifted by only 10 cm^{-1} to higher energy from that of [PPN][**4**], the cluster is considered to be predominantly anionic in character. The IR data are compatible with the $^{31}P\{^1H\}$ NMR data for THF and CH_2Cl_2 solutions of $[HNEt_3][\mathbf{4}]$. In THF solution, the spectrum resembles that of [PPN][**4**], where two doublets are observed at δ 528 and 281 with a ^2J(P,P) value of 29 Hz. At −90 °C in CD_2Cl_2, the resonance for the naked phosphorus is shifted upfield to δ 431 and displays a slightly reduced ^2J(P,P) value of 23 Hz. Although the μ_3-PH chemical shift of $[Et_3NH][\mathbf{4}]$ (δ 286) remains in the same region as that of the $[PPN]^+$ salt, the

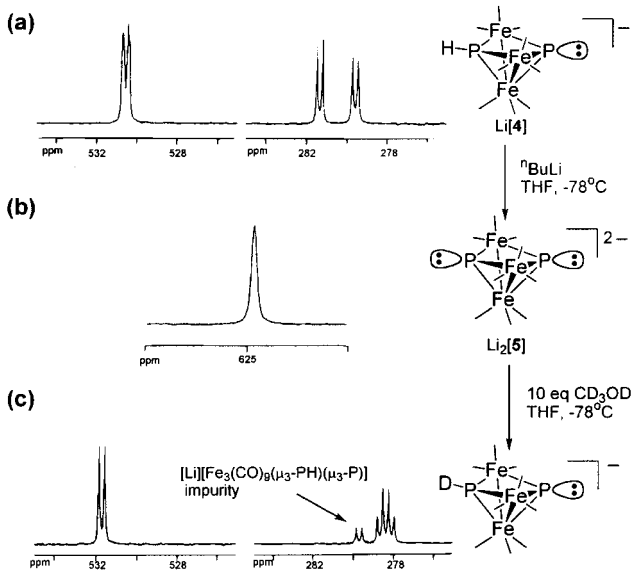

Figure 4. ^{31}P NMR Spectra of (a) $Li[Fe_3(CO)_9(\mu_3\text{-}PH)(\mu_3\text{-}P)]$ (Li[**4**]) (THF-d_8), (b) $Li_2[Fe_3(CO)_9(\mu_3\text{-}P)_2]$ (Li_2[**5**]) (THF), and (c) $^{31}P\{^1H\}$ NMR of $Li[Fe_3(CO)_9(\mu_3\text{-}PD)(\mu_3\text{-}P)]$ (THF-d_8).

^1J(H,P) value of 241 Hz is intermediate to that of **3** (338 Hz) and [PPN][**4**] (211 Hz). Warming the solution causes significant broadening of the resonances in the ^{31}P NMR spectrum resulting in a loss of resolvable ^2J(P,P) coupling; however, the chemical shifts of the peaks do not vary with temperature. At room temperature, decomposition is observed within 15 min, and several new resonances appear due to the instability of the anion in CH_2Cl_2 solution.

A very strong base, *n*-BuLi, is required to deprotonate the anion, $[Fe_3(CO)_9(\mu_3\text{-}PH)(\mu_3\text{-}P)]^-$ ($[\mathbf{4}]^-$), due to the difference in pK_a of the first and second protons of $Fe_3(CO)_9(\mu_3\text{-}PH)_2$ (**3**). Addition of 1 equiv of *n*-BuLi to **3** at −78 °C in THF produces Li[**4**] (eq 2). The energy of the CO stretches for the Li^+ salt of

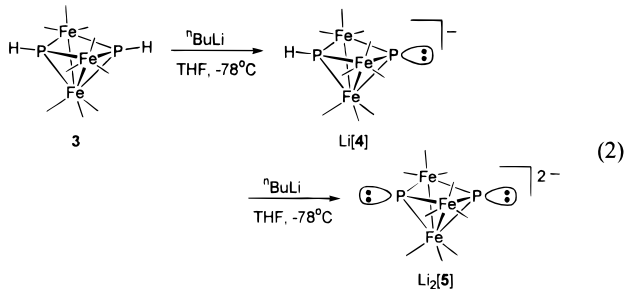

(2)

$[\mathbf{4}]^-$ are nearly identical to those for [PPN][**4**], indicating that Li^+ is not coordinated to phosphorus as it is observed to be in many lithium phosphides (Table 2).[20] After addition of a second equivalent of *n*-BuLi to Li[**4**] at −78 °C, a color change to a deep orange-brown is observed, and a new species is observed in the ^{31}P NMR spectrum with a broad singlet at δ 616.2 (−60 °C) (see Table 1, Figure 4b). The new species has a pattern similar to Li[**4**] in the infrared spectrum; however, the energies of the CO stretches are shifted to lower energy by 47 cm^{-1} to 1955 cm^{-1} (Figure 3a, Table 2). On the basis of the ^{31}P NMR and IR data, this species is assigned to the dianion, $Li_2[Fe_3$-

(20) See, for example: (a) Jones, R. A.; Stuart, A. L.; Wright, T. C. *J. Am. Chem. Soc.* **1983**, *105*, 7459−7460. (b) Hitchcock, P. B.; Lappert, M. F.; Power, P. P.; Smith, S. J. *J. Chem. Soc., Chem. Commun.* **1984**, 1669−1670. (c) Hey, E.; Hitchcock, P. B.; Lappert, M. F.; Rai, A. K. *J. Organomet. Chem.* **1987**, *325*, 1−12. (d) Bartlett, R. A.; Olmstead, M. M.; Power, P. P. *Inorg. Chem.* **1986**, *25*, 1243−1247.

$(CO)_9P_2]$ (Li_2[**5**]).[21] The doubly deprotonated species can be quenched by the addition of 10 equiv of CD_3OD to a THF solution of Li_2[**5**] to generate $[Fe_3(CO)_9(\mu_3\text{-PD})(\mu_3\text{-P})]^-$,[22] restoring the infrared spectrum in the CO stretching region and the color to that of [**4**]$^-$. The quartet splitting expected for the μ_3-PD phosphinidene cap is observed in the $^{31}P\{^1H\}$ NMR spectrum (Figure 4c). This differentiation in reactivity between the first and second cluster site permits reaction chemistry to be sequentially performed at each of the phosphorus atoms. All attempts to isolate the anionic clusters have not been successful thus far.

Alkylation. Deprotonation of $Fe_3(CO)_9(\mu_3\text{-}PH)_2$ (**3**) allows access to a phosphorus lone pair, which acts as a nucleophile toward organic electrophiles. Although neutral **3** is unreactive to $MeOSO_2CF_3$, reaction of a −78 °C CH_2Cl_2 solution of $[Et_3NH][Fe_3(CO)_9(\mu_3\text{-}PH)(\mu_3\text{-}P)]$ ([Et_3NH][**4**]) with 1 equiv of $MeOSO_2CF_3$ produces $Fe_3(CO)_9(\mu_3\text{-}PMe)(\mu_3\text{-}PH)$ (**6**) as the primary product (Scheme 3, Tables 1 and 2). The other products observed in the methylation reaction are the disubstituted cluster, $Fe_3(CO)_9(\mu_3\text{-}PMe)_2$ (**7**)[23] and **3**, where the ratio of **6**:**7**:**3** is 2:1:1. Pure **6** can be separated from the mixture by chromatography and is isolated as orange-red crystals in 54% yield. Changing the methylating agent to methyl iodide and varying the reaction temperature, concentration, or solvent only serve to increase the ratio of dimethyl to monomethyl product. Methylation of [PPN][**4**] yields only the bis-methylated product, **7**, and an unidentified tricluster oxidation product,[24] suggesting that the $HNEt_3^+$ counterion, which engages in hydrogen-bonding, is necessary to protect the phosphorus lone pair from oxidative side reactions.

The formation of $Fe_3(CO)_9(\mu_3\text{-}PMe)_2$, (**7**), from a simple deprotonation/alkylation sequence is unexpected given the difference in pK_a's for the two PH sites in $Fe_3(CO)_9(\mu_3\text{-}PH)_2$. A proton-transfer equilibrium between the product cluster $Fe_3(CO)_9(\mu_3\text{-}PMe)(\mu_3\text{-}PH)$, **6**, and $[Fe_3(CO)_9(\mu_3\text{-}PH)(\mu_3\text{-}P)]^-$ [**4**]$^-$ (eq 3) is expected to lie to the left, and IR and ^{31}P NMR data

$$\mathbf{6} + [Fe_3(CO)_9(\mu_3\text{-}PH)(\mu_3\text{-}P)]^- ([\mathbf{4}]^-) \underset{}{\overset{K<1}{\rightleftharpoons}} [Fe_3(CO)_9(\mu_3\text{-}PMe)(\mu_3\text{-}P)]^- ([\mathbf{8}]^-) + \mathbf{3} \qquad (3)$$

support this expectation.[25] To gain further insight into the methylation reaction, a low temperature ^{31}P NMR experiment was carried out on a solution containing [**4**]$^-$ and **6**, the two species expected to be present at an intermediate point in the methylation reaction. Upon cooling the solution to −90 °C, a color change to dark brown is observed. In addition to resonances for [**4**]$^-$ and **6**, four new resonances appear that are assigned to a P−P bonded dicluster adduct, [**9**]$^-$, on the basis of spectroscopic characterization (see Scheme 3).[26] The formation of dicluster [**9**]$^-$ is rationalized as a nucleophilic attack by the phosphorus lone pair of the methyl-capped anion, [**8**]$^-$, on the phosphorus site of the bicapped P−H cluster, **3**. Nucleophilic attack at the phosphorus site in a phosphinidene cluster finds precedence in the addition of hydride to $Fe_3(CO)_9(\mu_3\text{-}PPh)_2$. Fe−P bond cleavage is observed to produce the anionic phosphido complex, $[Fe_3(CO)_9(\mu_3\text{-}PPh)(\mu\text{-}P(H)Ph)]^-$.[27] Even though the equilibrium in (3) lies to the left, adduct formation is favored between the more nucleophilic phosphorus anion and the more electrophilic PH phosphinidene. The ^{31}P NMR resonances for [**9**]$^-$ disappear upon warming of the solution to 20 °C and return after recooling the sample to −90 °C. If *n*-BuLi is employed as the base to generate [**4**]$^-$, the low temperature ^{31}P NMR spectrum shows only resonances for [**9**]$^-$, indicating that formation of the hydrogen bonded adduct, [Et_3NH][**4**], competes with the formation of [**9**]$^-$.

At −90 °C, a ^{31}P NMR spectrum of the methylation reaction mixture of [Et_3NH][**4**] and $MeOSO_2CF_3$ in tetrahydrofuran solution shows resonances for the dicluster complex, [**9**]$^-$, indicating that it could play a role in determining the product distribution. Dissociation of the dicluster [**9**]$^-$ as the methyl-capped cluster monoanion, [**8**]$^-$, and **3** (as depicted in Scheme 3) followed by reaction with $MeOSO_2CF_3$ would lead to formation of the bis-methylated cluster, **7**. The details surrounding the formation of [**9**]$^-$ and its implication in the formation of **7** are complex. A complete discussion of the ^{31}P NMR characterization of [**9**]$^-$ and a related derivative is provided in the Supporting Information.

The deprotonation of $Fe_3(CO)_9(\mu_3\text{-}PMe)(\mu_3\text{-}PH)$ (**6**) with NEt_3/[PPN]Cl to yield $[PPN][Fe_3(CO)_9(\mu_3\text{-}PMe)(\mu_3\text{-}P)]$ [PPN]-[**8**] occurs in a facile manner similar to the deprotonation of $Fe_3(CO)_9(\mu_3\text{-}PH)_2$ (**3**) (see Tables 1 and 2). The CO stretches shift to lower energy by 50 cm^{-1}. The ^{31}P resonance for the naked phosphorus atom occurs at δ 513.1, which is 20 ppm upfield of the same phosphorus resonance in [PPN][**4**]. This spectrum exhibits a drastically reduced ^2J(P,P) value of 35 Hz as previously seen in the deprotonation of **3**. Prior to metathesis with [PPN]Cl, a hydrogen-bonded complex, $[Et_3NH][Fe_3(CO)_9(\mu_3\text{-}PMe)(\mu_3\text{-}P)]$, ([$Et_3NH$][**8**]) is observed in noncoordinating solvents, which displays spectroscopic behavior similar to that of [$HNEt_3$][**4**].

Oxidation. The lone pairs of organophosphine compounds are readily oxidized by group 16 elements to yield phosphine chalcogenides.[28] Similar reactivity is observed for metal clusters

(21) In the previous communication,[3c] we incorrectly concluded that the doubly deprotonated species contained a significant Li−P interaction since the ν_{CO} stretches were coincident with that of the monoanion, Li[**4**].

(22) The reaction mixture was produced by the addition of CD_3OD (8.0 μL, 0.20 mmol) to a 0.7 mL of THF solution of $Li_2Fe_3(CO)_9(\mu_3\text{-}P)_2$ (0.010 mmol) at −78 °C in a 5 mm NMR tube. $[Fe_3(CO)_9(\mu_3\text{-PD})(\mu_3\text{-P})]^-$: ^{31}P (δ, THF, −60 °C) 531.8 (dd, ^2J(P,P) = 34 Hz, μ_3-*P*) 278.4 (dt, ^2J(P,P) = 34 Hz, ^1J(D,P) = 34 Hz, μ_3-*P*D).

(23) Lang, H.; Zsolnai, L.; Huttner, G. *J. Organomet. Chem.* **1985**, *282*, 23−51.

(24) A tricluster species has been identified as a product resulting from the oxidation of $[Fe_3(CO)_9(\mu_3\text{-PH})(\mu_3\text{-P})]^-$ [**4**]$^-$ and is characterized by six resonances in the $^{31}P\{^1H\}$ NMR. $^{31}P\{^1H\}$ NMR (δ, CH_2Cl_2): 523 (P_A, ^2J(P,P) = 175), 274 (P_B, ^2J(P,P) = 175, ^1J(H,P) = 269), 167 (P_C, ^1J(P,P) = 333, ^2J(P,P) = 102, $^?J$(H,P) = 40), 145 (P_D, ^1J(P,P) = 333, ^2J(P, P) = 115, ^2J(P,P) = 85, ^1J(H,P) = 306, $^?J$(H,P) = 26, $^?J$(H,P) = 10), 98 (P_E, ^2J(P,P) = 115, ^1J(H,P) = 254, $^?J$(H,P) = 49), 46 (P_F, ^2J(P,P) = 115, ^2J(P,P) = 85, ^1J(H,P) = 250). A $^{31}P\{^1H\}$ NMR spectrum of this species is provided in the Supporting Information. The detailed structure of this product is not known.

(25) Experiments were conducted to gauge the relative basicities of [**4**]$^-$ and [**8**]$^-$. One equivalent of NEt_3 was added to 1 equiv each of $Fe_3(CO)_9(\mu_3\text{-}PMe)(\mu_3\text{-}PH)$ (**6**) and $Fe_3(CO)_9(\mu_3\text{-}PH)_2$ (**3**) in CH_2Cl_2 solution, and the resulting products were monitored by variable temperature ^{31}P NMR spectroscopy. In the ^{31}P NMR spectrum at −20 °C, very broad resonances for $[HNEt_3][Fe_3(CO)_9(\mu_3\text{-}PH)(\mu_3\text{-}P)]$ ([Et_3NH][**4**]) and $Fe_3(CO)_9(\mu_3\text{-}PMe)(\mu_3\text{-}PH)$ (**6**) are observed. The two species, [Et_3NH][**4**] and **6**, are also observed in a room-temperature IR spectrum of the reaction mixture. Thus, the predominant species observed in the reaction mixture support that the relative acidity of the P−H group in **3** is greater than that in **6** and $K < 1$. However, the broadening observed in the −20 °C ^{31}P spectrum suggests that the pK_a difference is not large enough to slow the proton exchange processes between **6** and [**4**]$^-$.

(26) ^{31}P NMR data (δ, CH_2Cl_2) for [**9**]$^-$: 369.1 (ddd, μ_3-P_A, $^1J(P_A,P_D)$ = 490, $^2J(P_A,JP_B)$ = 194, $^1J(H,P_A)$ = 32), 328.8 (dd, μ_3-P_BMe, $^2J(P_A,P_B)$ = 194, $^3J(P_B,P_D)$ = 43), 174.6 (dd, μ_3-P_CH, $^2J(P_C,P_D)$ = 294, $^1J(H,P_C)$ = 295), −64.4 (dddd, μ_3-P_DH, $^1J(P_A,P_D)$ = 490, $^2J(P_C,P_D)$ = 294, $^3J(P_B,P_D)$ = 43, $^1J(H,P_D)$ = 315). The chemical shift at δ −68 (P_D) is in the region observed for a phosphido ligand that bridges two nonbonding iron centers (ref 12). The other coupling constants are consistent with intracluster ^2J(P,P) values. Resonances at δ 183 and δ −68 display large couplings to directly bound hydrogens.

(27) Ohst, H. H.; Kochi, J. K. *Inorg. Chem.* **1986**, *25*, 2066−2074.

Scheme 4

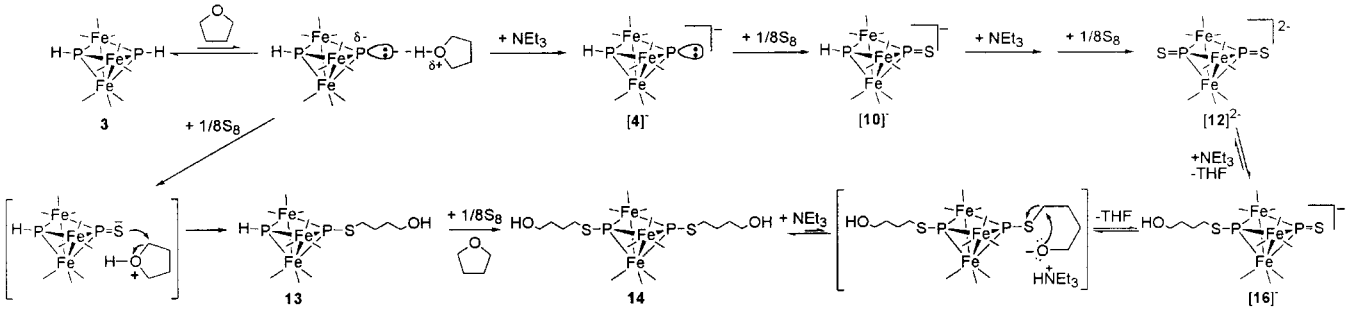

and several examples of cluster compounds containing μ_3-P═E (E = O, S, Se) caps have been reported.[29] The reactions of the cluster monoanions, $[HNEt_3][Fe_3(CO)_9(\mu_3\text{-}PH)(\mu_3\text{-}P)]$ ([**4**]$^-$) and $[HNEt_3][Fe_3(CO)_9(\mu_3\text{-}PMe)(\mu_3\text{-}P)]$ ([**8**]$^-$), as well as the neutral clusters, $Fe_3(CO)_9(\mu_3\text{-}PH)_2$ (**3**) and $Fe_3(CO)_9(\mu_3\text{-}PMe)(\mu_3\text{-}PH)$ (**6**), with elemental sulfur (S_8) have been investigated (Scheme 4); ^{31}P NMR and IR data are given in Tables 1 and 2. Reaction of [**4**]$^-$ with elemental sulfur (S_8) at −80 °C in THF solution cleanly produces the expected oxidation product, $[HNEt_3][Fe_3(CO)_9(\mu_3\text{-}PH)(\mu_3\text{-}P{=}S)]$ ([$HNEt_3$][**10**]), characterized by a pair of doublets at δ 230 (μ_3-PH) and δ 411 (μ_3-P═S) in the $^{31}P\{^1H\}$ NMR. The related methyl-capped cluster $[HNEt_3][Fe_3(CO)_9(\mu_3\text{-}PMe)(\mu_3\text{-}P{=}S)]$ ([$HNEt_3$][**11**]) is prepared by reaction of [**8**]$^-$ with S_8, and the product is observed as a pair of doublets at δ 321 (μ_3-PMe) and δ 406 (μ_3-P═S) in the $^{31}P\{^1H\}$ NMR spectrum. The intracluster ^2J(P,P) coupling values for clusters [**10**]$^-$ and [**11**]$^-$ are significantly larger (∼250 Hz) than for the parent cluster monoanions [**4**]$^-$ and [**8**]$^-$ (∼35 Hz). Deprotonation of cluster [$HNEt_3$][**10**] followed by addition of NEt_3 results in formation of the cluster dianion, $[HNEt_3]_2[Fe_3(CO)_9(\mu_3\text{-}P{=}S)_2]$ ($[HNEt_3]_2$[**12**]), whose symmetric μ_3-P═S caps appear as a singlet at δ 412 in the ^{31}P NMR.

The patterns of infrared CO stretches for the monoanions, [**10**]$^-$ and [**11**]$^-$, are nearly identical to those of the parent cluster anions, [**4**]$^-$ and [**8**]$^-$, but they are shifted 16 cm^{-1} to higher energy. Similarly, the pattern of the infrared CO stretches for the cluster dianion, Li_2[**12**], is nearly identical to the related cluster dianion, Li_2[**5**], but is shifted 38 cm^{-1} to higher energy (Table 2, Figure 3b). The infrared and ^{31}P NMR data reflect a small difference in the interaction for the cluster dianion, [**12**]$^{2-}$, with the two counterions, $HNEt_3^+$ and Li^+. The energy of the cluster core carbonyls is slightly lower (1994 vs 2002 cm^{-1}) and the phosphorus nuclei are shifted slightly downfield (420 vs 412 ppm) when Li^+ is the counterion instead of $HNEt_3^+$. The presence of a weak hydrogen-bonding interaction between the metallophosphine sulfide and the $HNEt_3^+$ counterion in THF solvent indicates that the interaction is stronger than that observed for [$HNEt_3$][**4**] and $[HNEt_3]_2$[**5**].

Two resonance structures can be drawn to describe the interaction between the phosphorus and sulfur atoms. Taking phosphorus as a four-electron donor, the $Fe_3(CO)_9$ core of the cluster dianion, [**12**]$^{2-}$, is considered neutral with the negative charges localized on the PS capping groups (eq 4). The degree

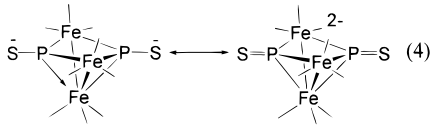

(4)

of π-bonding between the phosphorus and the electronegative sulfur atom can be inferred by comparison of the infrared data (ν_{CO}) for the sulfide clusters, [**10**]$^-$, [**11**]$^-$, and [**12**]$^{2-}$, and the parent clusters, [**4**]$^-$, [**8**]$^-$, and [**5**]$^{2-}$. If the negative charge is localized on the sulfur atoms, the cluster core carbonyls would appear at high energy, similar to the neutral clusters. However, electron donation from the sulfur to the phosphorus atom, forming a P═S bond, would increase the electron density felt by the cluster core carbonyl and give rise to an infrared spectrum low in energy near that of the parent clusters with a phosphorus lone pair. The infrared data for both the cluster monoanions, [**10**]$^-$ and [**11**]$^-$, as well as the bis-sulfido capped cluster, [**12**]$^{2-}$, show that the proportion of negative charge at the cluster core is roughly half that observed for the cluster when sulfur is not present to accept charge. On the basis of this analysis, the cluster chalcogenide PS bond is best described as intermediate between the single- and double-bonded representations shown above.

Reaction of the neutral clusters, **3** and **6**, with S_8 in THF solution without added base produces the clusters $Fe_3(CO)_9(\mu_3\text{-}PH)(\mu_3\text{-}PSCH_2CH_2CH_2CH_2OH)$ (**13**), $Fe_3(CO)_9(\mu_3\text{-}PSCH_2CH_2CH_2CH_2OH)_2$ (**14**), and $Fe_3(CO)_9(\mu_3\text{-}PMe)(\mu_3\text{-}PSCH_2CH_2CH_2CH_2OH)$ (**15**), with a ring-opened THF molecule appended to sulfur. The initial formulation of **13**−**15** was established by FAB-MS, and confirmed by spectroscopic characterization. Remarkably, only a slight shift of the strongest carbonyl band to lower energy is observed in the infrared spectrum in comparison to the parent phosphinidene cluster **3** (Table 2, Figure 3b). The ^{31}P resonances for the μ_3-PSR ligands are shifted upfield (δ ∼355) in comparison to the μ_3-PS$^-$ ligands (δ ∼410), and show intracluster coupling (^2J(P,P) ∼270) as well as coupling to two protons (^3J(P,H) = 6). Four resonances are observed in the ^{1}H NMR spectrum corresponding to the four methylene units of the ring-opened THF molecule (see Table 1).[30]

(28) Hudson, H. R. Nucleophilic Reactions of Phosphines. In *The Chemistry of Organophosphorus Compounds*; Hartley, F. R., Ed.; The Chemistry of Functional Groups Series; Wiley and Sons: Chichester, 1990; Vol. 1, pp 385−471.

(29) For (μ_3-P═O) capped clusters, see: (a) Davies, J. E.; Klunduk, M. C.; Mays, M. J.; Raithby, P. R.; Shields, G. P.; Tompkin, P. K. *J. Chem. Soc., Dalton Trans.* **1997**, 715−719. (b) Wang, W.; Corrigan, J. F.; Doherty, S.; Enright, G. D.; Taylor, N. J.; Carty, A. J. *Organometallics* **1996**, *15*, 2770−2776 and Corrigan, J. F.; Doherty, S.; Taylor, N. J.; Carty, A. J. *J. Am. Chem. Soc.* **1994**, *116*, 9799−9800. (c) Foerstner, J.; Olbrich, F.; Butenschön, H. *Angew. Chem., Int. Ed. Engl.* **1996**, *35*, 1234−1237. (d) Scherer, O. J.; Braun, J.; Walther, P.; Heckmann, G.; Wolmershäuser, G. *Angew. Chem., Int. Ed. Engl.* **1991**, *30*, 852−854. For (μ_3-P═S) clusters, see: (a) Lorenz, I.-P.; Pohl, W.; Polborn, K. *Chem. Ber.* **1996**, *129*, 11−13. (b) Davies, J. E.; Mays, M. J.; Pook, E. J.; Raithby, P. R.; Tompkin, P. K. *Chem. Commun.* **1997**, 1997−1998. (c) Vizi-Orosz, A.; Pályi, G.; Markó, L. *J. Organomet. Chem.* **1973**, *60*, C25−C26. (d) Foerstner, J.; Olbrich, F.; Butenschön, H. *Angew. Chem., Int. Ed. Engl.* **1996**, *35*, 1234−1237. (e) Grossbruchhaus, V.; Rehder, D. *Inorg. Chim. Acta* **1988**, *141*, 9−10. (f) Scherer, O. J.; Vondung, C.; Wolmershäuser, G. *Angew. Chem., Int. Ed.* **1997**, *36*, 1303−1305. For (μ_3-P═Se) clusters, see: Weigel, S.; Wolmershäuser, G.; Scherer, O. J. *Z. Anorg. Allg. Chem.* **1998**, *624*, 559−560.

Ring-opening of THF occurs upon interaction of a strong Brønsted or Lewis acid with the oxygen to form a cationic tertiary oxonium ion, which is activated to nucleophilic attack at the α-carbon.[31] The THF ring-opening initiator can be a simple acid, an electrophilic phosphine (PBr_3),[32] a Lewis acidic transition metal[33] or a lanthanide[34] complex. A proposed mechanism for the formation of the cluster-bound ring-opened THF species **13**−**15** is shown in Scheme 4. Infrared data show that clusters **3** and **6** are partially deprotonated by THF in solution, exposing the phosphorus lone pair to sulfur oxidation. The associated THF molecule becomes protonated and thus, activated toward nucleophilic attack at the α-carbon by the negatively charged metallophosphine chalcogenide, producing clusters **13**−**15**. Surprisingly, addition of 1 equiv of NEt_3 to the double ring-opened cluster, **14**, at −80 °C in THF results in a mixture of products including cluster **14**, $[HNEt_3][Fe_3(CO)_9(\mu_3\text{-}PSCH_2CH_2CH_2CH_2OH)(\mu_3\text{-}P{=}S)]$ $[HNEt_3][\mathbf{16}]$[35] and the cluster dianion, $[HNEt_3]_2[Fe_3(CO)_9(\mu_3\text{-}P{=}S)_2]$ ($[HNEt_3]_2[\mathbf{12}]$). Further addition of base results in a mixture containing only $[\mathbf{16}]^-$ and $[\mathbf{12}]^{2-}$; however, complete conversion to $[\mathbf{12}]^{2-}$ was not possible even after addition of a large excess of NEt_3.

Although the PSH-capped clusters are not isolable, the isolobal derivative in which the hydrogen is replaced by a gold phosphine moiety can be prepared (eq 5). Reaction of cluster **3**

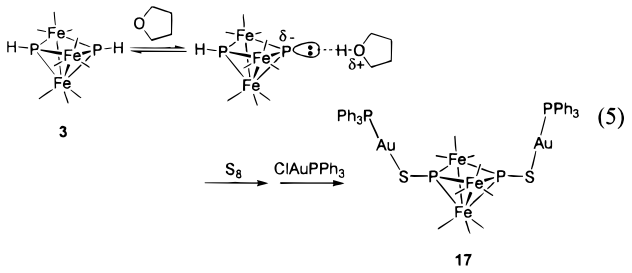

(5)

with S_8 in the presence of $ClAuPPh_3$ results in formation of $Fe_3(CO)_9(\mu_3\text{-}PSAuPPh_3)_2$ (**17**). Complex **17** is isolated as red needles, and its structure was determined by a single-crystal X-ray diffraction study (Figure 5, Table 3). The metric parameters of the Fe_3P_2 array are very similar to those of **3** (Table 3). The P−S distance of ∼2.06 Å, Au−S distance of ∼2.31 Å, and P−Au−S bond angle of 175.7° are similar to values reported for organophosphine sulfide complexes containing P−S−Au−P interactions.[36] The P−S−Au bond angles of 96.9° and 94.9° are slightly smaller than the values reported in the literature (96.2°−112.3°).

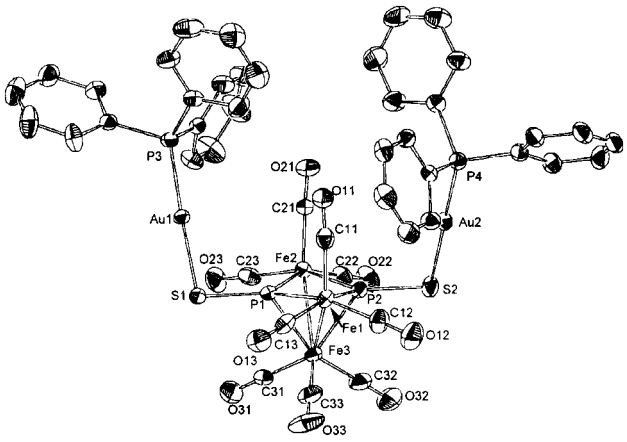

Figure 5. Diagram of $Fe_3(CO)_9(\mu_3\text{-}PSAuPPh_3)_2$ (**17**) showing the thermal ellipsoids (50% probability level) and the atomic labeling scheme.

Addition of Activated Alkenes. Primary and secondary organophosphines insert activated alkenes into the P−H bond without an added catalyst.[28] The P−H bonds in the neutral cluster, **3**, similarly react with acrylonitrile or methyl acrylate to yield single or double addition products, depending on the reaction stoichiometry (eq 6). The unsymmetrical compounds

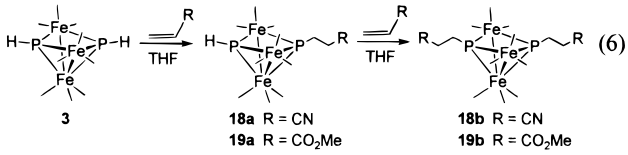

(6)

$Fe_3(CO)_9(\mu_3\text{-}PH)(\mu_3\text{-}P(CH_2)_2R)$ (R = CN; **18a**, CO_2Me; **19a**) show a pair of doublets in the $^{31}P\{^1H\}$ NMR spectrum at δ 235.3, 321.4 ($^2J(P,P) = 315$) and δ 234.7, 337.0 ($^2J(P,P) = 313$), respectively. Singlet resonances are observed for the two symmetric products, $Fe_3(CO)_9(\mu_3\text{-}P(CH_2)_2R)_2$ (R = CN (**18b**), CO_2Me (**19b**)), by $^{31}P\{^1H\}$ NMR at δ 320.6 and δ 335.2 (Table 1), slightly upfield from the value of δ 343 observed for related cluster, $Fe_3(CO)_9(\mu_3\text{-}PEt)_2$.[37] The infrared patterns observed in the CO stretching region for the symmetric clusters **18b** and **19b** are nearly identical to that observed for the parent cluster, **3**, but are shifted to slightly lower energy (2047 cm^{-1} (**3**), 2043 cm^{-1} (**18b**), and 2040 cm^{-1} (**19b**)) (Table 2). The solid-state structure of the double-insertion product, **18b**, was confirmed by a single-crystal X-ray diffraction study (Figure 6, Table 3). The two pendant $P(CH_2)_2CN$ ligands cap the open Fe_3P_2 array. The metric parameters of the Fe_3P_2 core are very similar to other derivatives (Table 3). The mechanism for the formation of the olefin insertion products in organophosphines involves nucleophilic attack of the phosphorus lone pair on the activated double bond. In the case of the cluster reactions, partial deprotonation of **3** by a THF molecule can provide access to a nucleophilic phosphorus. The hypothesis that a deprotonated cluster is the active species is supported by the fact that reaction of the P−H

(30) The connectivity of the resonances in the ^1H NMR spectrum was established from $^1H\{^{31}P\}$ NMR and 2D COSY experiments.

(31) (a) Penczek, S.; Kubisa, P.; Matyjaszewski, K. *Adv. Polym. Science* **1980**, *37*, 1−144. (b) Ledwith, A.; Sherrington, D. C. *ibid.* **1975**, *19*, 1−56. (c) Dreyfuss, P.; Dreyfuss, M. P. *Compr. Chem. Kinet.* **1976**, *15*, 259.

(32) Hinke, A.; Kuchen, W. *Z. Naturforsch.* **1982**, *37b*, 1543−1547.

(33) (a) Polamo, M.; Mutikainen, I.; Leskela, M. *Acta Crystallogr.* **1997**, *C53*, 1036−1037. (b) Breen, T. L.; Stephen, D. W. *Inorg. Chem.* **1992**, *31*, 4019−4022. (c) Boisson, C.; Berthet, J. C.; Lance, M.; Nierlich, M.; Ephritikhine, M. *Chem. Commun.* **1996**, 2129−2130. (d) Borkowsky, S. L.; Jordan, R. F.; Hinch, G. D. *Organometallics* **1991**, *10*, 1268−1274. (e) Okuda, F.; Watanabe, Y. *Bull. Chem. Soc. Jpn.* **1990**, *63*, 1201. (f) Oku, A.; Homoto, Y.; Harada, T. *Chem. Lett.* **1986**, 1495−1498. (g) Tsuji, Y.; Kobayashi, M.; Okuda, F.; Watanabe, Y. *J. Chem. Soc., Chem. Commun.* **1989**, 1253−1254.

(34) (a) Harwood, L. M.; Jackson, B.; Prout, K.; Witt, F. J. *Tetrahedron Lett.* **1990**, *31*, 1885−1888. (b) Evans, W. J.; Ulibarri, T. A.; Chamberlain, L. R.; Ziller, J. W.; Alvarez, D., Jr. *Organometallics* **1990**, *9*, 2124−2130. (c) Schumann, H.; Palamidis, E.; Loebel, J. *J. Organomet. Chem.* **1990**, *384*, C49−C52. (d) Avens, L. R.; Barnhart, D. M.; Burns, C. J.; McKee, S. D. *Inorg. Chem.* **1996**, *35*, 537−539.

(35) Cluster $[HNEt_3][Fe_3(CO)_9(\mu_3\text{-}PSCH_2CH_2CH_2CH_2OH)(\mu_3\text{-}P{=}S)]$ ($[HNEt_3][\mathbf{16}]$) is identified on the basis of the similarity of the ^{31}P NMR and IR data to clusters $[\mathbf{10}]^-$ and $[\mathbf{11}]^-$ (See Tables 1 and 2, Figure 3b).

(36) (a) Staples, R. J.; Wang, S.; Fackler, J. P., Jr.; Grim, S. O.; de Laubenfels, R. *Acta Crystallogr., Sect. C.* **1994**, *50*, 1242. (b) Preisenberger, M.; Schier, A.; Schmidbaur, H. *Z. Naturforsch., Teil B.* **1998**, *53*, 781−787. (c) Preisenberger, M.; Bauer, A.; Schmidbaur, H. *Chem. Ber.* **1997**, *130*, 955−958. (d) Murray, H. H.; Garzón, G.; Raptis, R. G.; Mazany, A. M.; Porter, L. C.; Fackler, J. P., Jr. *Inorg. Chem.* **1988**, *27*, 836−842. (e) Usón, R.; Laguna, A.; Laguna, M.; Fraile, M. N.; Lázaro, I.; Gimeno, M. C.; Jones, P. G.; Reihs, C.; Sheldrick, G. M. *J. Chem. Soc., Dalton Trans.* **1990**, 333.

(37) From unpublished results. The ethyl-capped cluster, $Fe_3(CO)_9(\mu_3\text{-}PEt)_2$, is obtained by reaction of the cluster anion, $[\mathbf{4}]^-$, with EtOTf in an analogous reaction to that reported for $Fe_3(CO)_9(\mu_3\text{-}PMe)_2$ (**7**).

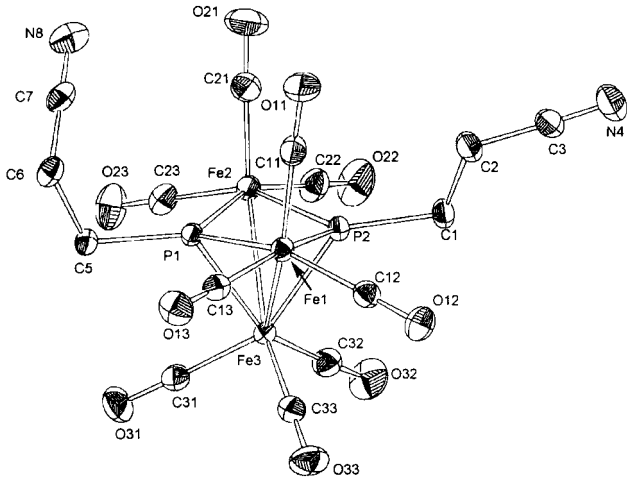

Figure 6. Diagram of $Fe_3(CO)_9(\mu_3\text{-}PCH_2CH_2CN)_2$ (**18b**) showing the thermal ellipsoids (50% probability level) and the atomic labeling scheme.

capped cluster, **3**, with acrylonitrile proceeds considerably slower in CH_2Cl_2 (days) than in THF (min).

Conclusions

The cluster, $Fe_3(CO)_9(\mu_3\text{-}PH)_2$ (**3**), prepared by hydrolysis of the silylphosphinidene cluster, $Fe_3(CO)_9[\mu_3\text{-}PSi(i\text{-}Pr)_3]_2$ (**2**), is the first example of a bifunctional cluster containing two reactive P−H sites. The two sites share the same pool of cluster electrons, and accordingly, modification of one P−H site affects the reactivity of the second P−H site. Similar to organophosphines, the deprotonated clusters $[\mathbf{4}]^-$ and $[\mathbf{8}]^-$, with reactive phosphorus lone pairs, are readily alkylated and oxidized by sulfur. Likewise, activated olefins insert into the two P−H bonds as observed for primary organophosphines, RPH_2. In all cases, unsymmetrical products, in which only one of the cluster caps has reacted, can be prepared. The ability to perform stepwise reactions is required to control chain length in the synthesis of cluster materials based on the Fe_3P_2 building block. We will report soon on our studies that take advantage of this selective reaction chemistry to prepare oligomers of redox-active clusters linked by coordination to square-planar transition metal complexes.[7d]

Experimental Section

Materials and Methods. Hexanes, pentane, tetrahydrofuran (THF), toluene, glyme, and diethyl ether were freshly distilled from sodium benzophenoneketyl radical (purple solutions) prior to use. Methanol was distilled from sodium methoxide, dichloromethane was distilled from P_2O_5, and triethylamine was distilled from CaH_2. Trimethylsilyl chloride and triisopropylsilyl chloride (Aldrich) were distilled from poly(4-vinylpyridine) (Reillex 402, Aldrich) immediately before use. The counterion source, [PPN]Cl ($[PPN]^+ = (Ph_3P)_2N^+$, Johnson-Matthey), was recrystallized from distilled water and dried at 140 °C before use. Aluminum trichloride (Aldrich) was sublimed through aluminum before use. Methyl trifluoromethanesulfonate ($MeOSO_2CF_3$), iron pentacarbonyl (2.2 M in hexanes, Alfa), and methyl acrylate (Aldrich) were vapor-distilled before use. Phosphine gas (Pfaltz and Bauer), *n*-butyllithium (Alfa), iron dodecacarbonyl ($Fe_3(CO)_{12}$, Strem), elemental sulfur (S_8, Aldrich), acrylonitrile (Aldrich), Florosil (Fisher), and Kieselgel 60 (Fluka) were all used as received. Monolithium phosphide, $LiPH_2$·glyme, was prepared following a literature procedure.[38] All chromatography was performed under a nitrogen atmosphere, and the eluting solvents were dried over 4 Å Linde molecular sieves. All of the compounds are air-sensitive and were either handled under an inert atmosphere using standard Schlenk techniques or manipulated in a nitrogen atmosphere drybox.

The ^1H and ^{31}P NMR spectra were obtained on Bruker AC200, Bruker WM250, Bruker AMX300, Varian 300 (NMRUGLY), or Varian XL400 spectrometers. All ^1H chemical shifts were reported as positive downfield from tetramethylsilane and recorded on the above instruments operating at 200.133, 250.133, 300.133, and 399.875 MHz, respectively. The ^{31}P NMR spectra were performed with the use of deuterated or nondeuterated solvents, and the chemical shifts were referenced to H_3PO_4 (RT) or $P(OMe)_3$ (LT) externally on the above instruments operating at 81.015, 101.256, 121.496, and 161.876 MHz, respectively. The concentrations of phosphorus-containing products were calculated by integrating the ^{31}P NMR resonances of a solution containing the desired compound versus a concentric tube containing an internal standard ($P(OMe)_3$) of known concentration. Both the internal standard and the sample had $Cr(acac)_3$ added to a concentration of 0.1 M to act as a relaxation agent and to suppress the nuclear Overhauser enhancement so that correct integrations could be obtained. All NMR simulations were performed with the use of either LAOCN5 (Quantum Chemistry Program Exchange, No. QCMP 049) or GNMR (Cherwell Scientific). Infrared spectra were recorded on a Bomem Michelson 120 Fourier transform infrared spectrometer. Elemental analyses were performed by Pascher Microanalytical Laboratories (Remagen, Germany) and Oneida Research Services (Whitesboro, New York). Fast atom bombardment (FAB) mass spectrometry by means of a high-resolution JEOL HX-110 mass spectrometer (NBA matrix) was performed at the North Carolina State University Mass Spectrometry Facility (Raleigh, North Carolina).

Preparation of $H_2PSi(i\text{-}Pr)_3$. This synthesis is an adaptation of the method of Schäfer.[39] A solution of aluminum trichloride (1.3 g, 9.8 mmol, sublimed) in 10 mL of Et_2O was cannulated dropwise over a period of 2−3 min into a solution of $LiPH_2$·glyme (5.0 g, 0.038 mol) in 30 mL of glyme. After the mixture stirred for 30 min at room temperature, freshly distilled triisopropylsilyl chloride (4.9 mL, 0.023 mol) was added at 0 °C. The suspension was stirred for 48 h to ensure complete reaction. The salts were filtered off and washed with 2 × 5 mL of Et_2O. The filtrate was placed in a warm water bath, and the Et_2O and glyme were removed under vacuum for 3−4 h to avoid contamination of low-boiling impurities in the volatile final product. The $H_2PSi(i\text{-}Pr)_3$ was vapor-distilled as a colorless liquid. The volume faction of $H_2PSi(i\text{-}Pr)_3$ versus other volatiles was determined by ^1H NMR (5 mL, 90% yield). ^1H NMR (δ, $CDCl_3$) 1.15 (multiplet, $PSi[CH(CH_3)_2]_3$) 1.05 (apparent d, $PSi[CH(CH_3)_2]_3$) 0.95 ($^1J(H,P) = 188$, H_2P). $^{31}P\{^1H\}$ NMR (δ, toluene) −276 s.

Preparation of $Fe_3(CO)_9(\mu_3\text{-}PH)_2$ (3). A solution of $Fe_3(CO)_{12}$ (2.53 g, 5.03 mmol) and $H_2PSi(i\text{-}Pr)_3$ (1.09 mL of a 97.6% solution in glyme, 5.03 mmol) in 125 mL of toluene was heated at 60 °C for 2 h and a color change from dark green to red-brown was observed. The $^{31}P\{^1H\}$ NMR spectrum in toluene shows a single peak at δ 378 corresponding to the monocapped phosphinidene cluster, $Fe_3(CO)_9(\mu\text{-}CO)[\mu_3\text{-}PSi(i\text{-}Pr)_3]$ (50−60% solution yield). A second portion of $H_2PSi(i\text{-}Pr)_3$ (1.013 mL of a 94.5% solution in glyme, 4.53 mmol) was added, and the solution was heated at 60 °C for 1 h, and then at 90 °C for an additional 3 h. The major product in the $^{31}P\{^1H\}$ NMR spectrum of the red-brown solution was the bicapped phosphinidene cluster, $Fe_3(CO)_9[\mu_3\text{-}PSi(i\text{-}Pr)_3]_2$ (**2**) (δ 280, 40% solution yield). An excess of degassed deionized water was added (2.0 mL, 0.111 mol) and the solution was stirred for 1 h. After the volatiles were removed under vacuum, the resulting dark brown oil was dissolved in 5 mL of CH_2Cl_2. Addition of 150 mL of hexanes resulted in precipitation of an insoluble material which was removed by filtration and washed with hexanes (2 × 50 mL). The solvent was removed under vacuum, and the resulting orange-red solid was dissolved in 4 mL of 1:1 CH_2Cl_2:hexanes and loaded atop a 1.5 in × 6 in fluorosil column. A red band was collected in hexanes until a brown-purple band, corresponding to the mono-capped cluster $Fe_3(CO)_9(\mu\text{-}CO)(\mu_3\text{-}PH)$, started to elute. After removal of solvent, a red-orange powder was recovered and recrystallized from concentrated hexanes at 0 °C (red-brown crystalline solid,

(38) Schäfer, H.; Fritz, G.; Hölderich, W. *Z. Anorg. Allg. Chem.* **1977**, *428*, 222−224.

(39) Fritz, G.; Schäfer, H. *Z. Anorg. Allg. Chem.* **1971**, *385*, 243−255.

0.664 g, 30% yield). ^{1}H NMR (δ, toluene-d_8) 4.07 (AA′, $|^1J(H,P)| = 316$, $|^3J(H,P)| = 14$, $|^4J(H,H)| = 9$, $|^2J(P,P)| = 338$, μ_3-P*H*); IR (ν_{PH}, Nujol mull) 2327 (vw), 2314 (vw). Anal. Calcd (found) for $C_9H_2Fe_3O_9P_2$: C, 22.35 (22.71); H, 0.42 (0.51).

Generation of [PPN][$Fe_3(CO)_9(\mu_3\text{-}PH)(\mu_3\text{-}P)$] ([PPN][4]). Samples of $Fe_3(CO)_9(\mu_3\text{-}PH)_2$ (**3**) (10.0 mg, 0.021 mmol), [PPN]Cl (11.8 mg, 0.021 mmol), and 2.5 mL of THF were added to a Schlenk flask. The red solution containing suspended [PPN]Cl was placed in a 0 °C bath, and NEt_3 (0.0028 mL, 0.020 mmol) was added; the solution color changed to an orange solution with a fine white precipitate upon NEt_3 addition. The volatiles were removed at 0 °C under vacuum, and the resulting orange oil was dissolved in 2 mL of Et_2O. The solution was filtered through Celite, and the Celite pad was washed with Et_2O. The product can be stored as an orange oil in a −15 °C freezer for 1−2 days. Solutions of the anion were stable in a −15 °C freezer for only a few hours. ^{1}H NMR (δ, THF-d_8) 6.28 (dd, $^1J(H,P) = 211$, $^3J(H,P) = 11$, μ_3-P*H*).

Generation of [$HNEt_3$][$Fe_3(CO)_9(\mu_3\text{-}PH)(\mu_3\text{-}P)$] ([$HNEt_3$][4]). A sample of $Fe_3(CO)_9(\mu_3\text{-}PH)_2$ (**3**) (10.0 mg, 0.021 mmol) was dissolved in 0.7 mL of CD_2Cl_2 in a 5 mm NMR tube. The NMR tube was placed in an acetone/dry ice bath and NEt_3 (0.0028 mL, 0.020 mmol) was added. No obvious color change was observed. The variable temperature ^{31}P NMR experiment was initiated at −90 °C since samples of [$HNEt_3$][**4**] decompose in dichloromethane solutions at room temperature.

Generation of Li[$Fe_3(CO)_9(\mu_3\text{-}PH)(\mu_3\text{-}P)$] (Li[4]). A sample of $Fe_3(CO)_9(\mu_3\text{-}PH)_2$ (**3**) (0.01 g, 0.021 mmol) was dissolved in 0.7 mL of THF in a 5 mm NMR tube. The tube was cooled in an acetone/dry ice bath, and *n*-BuLi (0.010 mL of a 2.06 M solution in *n*-hexanes, 0.010 mmol) was added. No obvious color change was observed. ^{1}H (δ, THF-d_8, −60 °C) 6.36 (dd, $^1J(H,P) = 216$, $^3J(H,P) = 10$, μ_3-P*H*); ^{31}P (δ, THF-d_8, −60 °C) 530.6 (dd, $^2J(P,P) = 34$, $^3J(H,P) = 10$, μ_3-*P*), 277.5 (dd, $^2J(P,P) = 34$, $^1J(H,P) = 216$, μ_3-*P*H); IR (ν_{CO}, THF) 2043 (vw), 2003 (vs), 1980 (s), 1956 (m), 1944 (sh).

Generation of Li_2[$Fe_3(CO)_9(\mu_3\text{-}P_2]$ (Li_2[5]). A sample of $Fe_3(CO)_9(\mu_3\text{-}PH)_2$ (10 mg, 0.021 mmol) was dissolved in 0.7 mL of THF in a 5 mm NMR tube. The tube was cooled in an acetone/dry ice bath and *n*-BuLi (0.020 mL of a 2.06 M solution in *n*-hexanes, 0.021 mmol) was added. The color immediately changed from orange-red to a dark orange-brown. Solutions of Li_2[**5**] were stable at room temperature for less than 1 h.

Preparation of $Fe_3(CO)_9(\mu_3\text{-}PMe)(\mu_3\text{-}PH)$ (6). A 40 mL CH_2Cl_2 solution of $Fe_3(CO)_9(\mu_3\text{-}PH)_2$ (**3**) (0.10 g, 0.21 mmol) was cooled in an acetone/CO_2 bath, and NEt_3 (0.029 mL, 0.21 mmol) was added, resulting in an immediate color change from red to dark brown. An aliquot of $MeOSO_2CF_3$ (0.022 mL, 0.22 mmol) was added, and the solution was stirred while the bath warmed to room temperature. Upon addition of $MeOSO_2CF_3$, the color of the solution turned a darker brown; however, by the time the bath reached −20 °C, the solution was red in color. A ^{31}P NMR spectrum of the reaction mixture showed an approximately 2:1:1 ratio of $Fe_3(CO)_9(\mu_3\text{-}PMe)(\mu_3\text{-}PH)$ (**6**):$Fe_3(CO)_9(\mu_3\text{-}PH)_2$ (**3**):$Fe_3(CO)_9(\mu_3\text{-}PMe)_2$ (**7**). The CH_2Cl_2 was removed under vacuum, and the residue was extracted into hexanes (10 mL). The hexanes solution was loaded onto a 1 in × 6 in column of pretreated silica gel 60. The pretreatment procedure consisted of rinsing the support with MeOH followed by acetone and then drying the support in a stream of nitrogen. Elution with hexanes yielded two orange bands: $Fe_3(CO)_9(\mu_3\text{-}PMe)_2$ (first) and $Fe_3(CO)_9(\mu_3\text{-}PMe)(\mu_3\text{-}PH)$ (second). Elution with CH_2Cl_2/hexanes (3:1) yielded $Fe_3(CO)_9(\mu_3\text{-}PH)_2$. Recrystallization of **6** from hexanes produced fine red needles (50 mg, 54% yield). Data for **6**: ^{1}H (δ, C_6H_6) 4.07 (dd, $^1J(H,P) = 315$, $^3J(H,P) = 14$, μ_3-P*H*), 1.62 (dd, $^2J(H,P) = 13$, $^4J(H,P) = 3$, μ_3-PC*H*$_3$); IR (ν_{PH}, Nujol mull) 2304 (vw). Anal. Calcd (found) for $C_{10}H_4Fe_3O_9P_2$: C, 24.14 (24.37); H, 0.81 (0.83). Data for **7**: ^{1}H (δ, C_6D_6) 1.69 (virtual t, $|^2J(H,P) + {}^4J(H,P)| = 15$, μ_3-PC*H*$_3$).

Generation of [PPN][$Fe_3(CO)_9(\mu_3\text{-}PMe)(\mu_3\text{-}P)$] ([PPN][8]). Samples of $Fe_3(CO)_9(\mu_3\text{-}PMe)(\mu_3\text{-}PH)$ (0.015 g, 0.030 mmol) and [PPN]Cl (0.018 g, 0.031 mmol) were dissolved in 2.5 mL of THF. The solution was placed in an ice bath, and NEt_3 (0.0042 mL, 0.030 mmol) was added. The originally red solution which had some insoluble [PPN]Cl particles changed to an orange solution with a fine white precipitate. The THF was removed under vacuum at 0 °C, and the resulting orange oil was dissolved in 2 mL of diethyl ether. The solution was filtered through Celite, leaving behind a white solid, and the Celite pad was washed with diethyl ether. The product can be stored as an orange oil in a −15 °C freezer for only 1−2 days. Solutions of the anion are stable in a −15 °C freezer for only a few hours. ^{1}H (δ, THF-d_8) 2.32 (d, $^2J(P,H) = 11$, μ_3-PC*H*$_3$).

Generation of [$HNEt_3$][$Fe_3(CO)_9(\mu_3\text{-}PH)(\mu_3\text{-}P{=}S)$] ([$HNEt_3$][10]). A sample of $Fe_3(CO)_9(\mu_3\text{-}PH)_2$ (**3**) (0.00629 g, 0.0130 mmol) was dissolved in 0.7 mL of THF in a 5 mm NMR tube containing elemental sulfur (S_8) (0.47 mg, 0.0147 mmol). The tube was cooled to − 78 °C in an acetone/CO_2 bath and 1.6 μL NEt_3 (0.0115 mmol) was added. The color darkened slightly from orange-red to orange-brown, corresponding to formation of [**4**]$^-$. Because of the insolubility of sulfur in THF, it was necessary to invert the NMR tube to aid in the reactivity. Formation of the product, [$HNEt_3$][$Fe_3(CO)_9(\mu_3\text{-}PH)(\mu_3\text{-}P{=}S)$], was confirmed by ^{31}P, ^{1}H NMR, and IR spectroscopy. ^{1}H (δ, THF-d_8) 5.05 (dd, $^1J(P,H) = 291$, $^3J(P,H) = 20$, μ_3-P*H*).

Generation of [$HNEt_3$][$Fe_3(CO)_9(\mu_3\text{-}PMe)(\mu_3\text{-}P{=}S)$] ([$HNEt_3$][11]). A sample of $Fe_3(CO)_9(\mu_3\text{-}PMe)(\mu_3\text{-}PH)$ (**6**) (0.00436 g, 0.00876 mmol) was dissolved in 8 mL of THF. The solution was cooled to 0 °C in an ice bath. Addition of 1.21 μL NEt_3 resulted in a slight darkening of the solution color corresponding to formation of the cluster anion, [$HNEt_3$][**8**]. The solution was cannulated into a flask containing elemental sulfur (0.49 mg, 0.0153 mmol). Formation of the product, [$HNEt_3$][$Fe_3(CO)_9(\mu_3\text{-}PMe)(\mu_3\text{-}P{=}S)$], was confirmed by ^{31}P NMR and IR spectroscopy.

Generation of [$HNEt_3$]$_2$[$Fe_3(CO)_9(\mu_3\text{-}P{=}S)_2$] ([$HNEt_3$]$_2$[12]). The cluster, $Fe_3(CO)_9(\mu_3\text{-}PH)_2$ (**3**) (0.0055 g, 0.0114 mmol), was dissolved in 0.7 mL of THF in a 5 mm NMR tube containing excess elemental sulfur. The tube was cooled in a dry ice/acetone bath. To the solution was added an excess of NEt_3, which initially caused a color change from red-orange to dark orange, corresponding to formation of [**4**]$^-$, but after several minutes the color turned red. Formation of the product, [$HNEt_3$]$_2$[$Fe_3(CO)_9(\mu_3\text{-}P{=}S)_2$] ([$HNEt_3$]$_2$[**12**]), was confirmed by ^{31}P NMR and IR spectroscopy.

Generation of $Fe_3(CO)_9(\mu_3\text{-}PH)(\mu_3\text{-}PS(CH_2)_4OH)$ (13) and $Fe_3(CO)_9(\mu_3\text{-}PS(CH_2)_4OH)_2$ (14). A 1 mL THF solution of $Fe_3(CO)_9(\mu_3\text{-}PH)_2$ (0.0086 g, 0.0178 mmol) was cannulated into a flask containing S_8 (0.53 mg, 0.0165 mmol). After the solution stirred for 2 h, the solution color became red-orange. A ^{31}P NMR spectrum of the reaction mixture showed two doublets, corresponding to the half-substituted product, $Fe_3(CO)_9(\mu_3\text{-}PH)(\mu_3\text{-}PS(CH_2)_4OH)$ (**12**). A second equivalent of sulfur was added (0.62 mg, 0.0193 mmol) to the solution. The solution color again became more red-orange, and the ^{31}P NMR spectrum showed a singlet, confirming formation of the product, $Fe_3(CO)_9(\mu_3\text{-}PS(CH_2)_4OH)_2$ (**14**). The reaction mixture was filtered through Celite to remove unreacted sulfur. Cluster **14** is stable in THF solution under nitrogen for several days; however, all attempts at isolation resulted in decomposition. ^{1}H (δ, THF-d_8) 3.05 (pt, $^3J(P,H) = 6.1$, $^3J(H,H) = 7.2$, μ_3-PSC*H*$_2$(CH$_2$)$_3$OH), 1.85 (pt, $^3J(H,H) = 7.2$, $^3J(H,H) = 7.0$, μ_3-PSCH$_2$C*H*$_2$(CH$_2$)$_2$OH), 1.58 (m, $^3J(H,H) = 7.0$, μ_3-PS(CH$_2$)$_2$C*H*$_2$CH$_2$OH), 3.71 (br, μ_3-PS(CH$_2$)$_3$C*H*$_2$OH); ^{13}C{^{1}H} (δ, THF-d_8): 62.0 (s, μ_3-PS(CH$_2$)$_3$*C*H$_2$OH), 40.7 (s, μ_3-PS(CH$_2$)$_2$*C*H$_2$CH$_2$OH), 32.9 (d, μ_3-PS*C*H$_2$(CH$_2$)$_3$OH, $^2J(P,C) = 10$), 28.4 (s, μ_3-PSCH$_2$*C*H$_2$(CH$_2$)$_2$OH); FAB-MS (NBA/THF) for $Fe_3(CO)_9(\mu_3\text{-}PS(CH_2)_4OH)_2$ (**14**): 692.7 (M^+H), 691.7 (M^+), 607.8 (M^+− 3CO), 523.8 (M^+ − 6CO), 495.7 (M^+ − 7CO), 467.8 (M^+ − 8CO), 439.8 (M^+− 9CO).

Generation of $Fe_3(CO)_9(\mu_3\text{-}PMe)(\mu_3\text{-}PS(CH_2)_4OH)$ (15). Synthesis of **15** is achieved by reaction of a THF solution of $Fe_3(CO)_9(\mu_3\text{-}PMe)(\mu_3\text{-}PH)$ and elemental sulfur in an analogous manner to **14**. ^{1}H (δ, THF-d_8) 3.03 (pt, $^3J(P,H) = 6$, μ_3-PSC*H*$_2$(CH$_2$)$_3$OH), 2.48 (dd, $^2J(P,H) = 12.6$, μ_3-PC*H*$_3$); FAB-MS (NBA/THF) for $Fe_3(CO)_9(\mu_3\text{-}PMe)(\mu_3\text{-}PS(CH_2)_4OH)_2$ (**15**): 602.7 (M^+H), 601.7 (M^+), 517.8 (M^+ − 3CO), 489.8 (M^+ − 4CO), 461.7 (M^+ − 5CO), 433.8 (M^+ − 6CO), 377.8 (M^+ − 8CO), 349.8 (M^+ − 9CO).

Generation of [$HNEt_3$][$Fe_3(CO)_9(\mu_3\text{-}PS(CH_2)_4OH)(\mu_3\text{-}P{=}S)$] ([$HNEt_3$][16]). A 5 mm NMR tube containing $Fe_3(CO)_9(\mu_3\text{-}PS(CH_2)_4OH)_2$ dissolved in 0.7 mL of THF was cooled in a dry ice/acetone bath. To the solution was added 1 equiv of NEt_3. Formation of the

product, $[HNEt_3][Fe_3(CO)_9(\mu_3\text{-}PS(CH_2)_4OH)(\mu_3\text{-}P{=}S)]$, was confirmed by ^{31}P NMR and IR spectroscopy.

Preparation of $Fe_3(CO)_9(\mu_3\text{-}PSAuPPh_3)_2$ (17). Reaction of the neutral cluster, $Fe_3(CO)_9(\mu_3\text{-}PH)_2$ (**3**) (0.0177 g, 0.0365 mmol), with excess elemental sulfur (0.005 g, 0.156 mmol) and $ClAuPPh_3$ (0.075 g, 0.0512 mmol) was carried out in 10 mL of THF. After stirring for 12 h, the solvent was removed, and the resulting oil was dissolved in a 2:1 mixture of toluene:THF and loaded onto a $^3/_4$ in $\times$ 6 in fluorosil column. The product, $Fe_3(CO)_9(\mu_3\text{-}PSAuPPh_3)_2$, was eluted with THF as an orange band. Recrystallization of **17** from THF/diethyl ether produced red needles (5.77 mg, 11% yield). ^{31}P NMR (δ, THF) 388 (s, μ_3-*P*SAuPPh$_3$), 40 (s, μ_3-PSAu*P*Ph$_3$); ^1H (δ, THF-d_8) ~7.5 (br, P(C_6H_5)$_3$); FAB-MS (NBA/THF) for **17**: 1464.9 (M^+H), 1409.6 ($M^+ - 2CO$), 1324.6 ($M^+ - 5CO$), 1267.9 ($M^+ - 7CO$), 1212.7 ($M^+ - 9CO$), 1147.1 ($M^+ - 2CO - PPh_3$), 951.0 ($M^+ - 9CO - PPh_3$). Anal. Calcd (found) for $C_{45}H_{30}Au_2Fe_3O_9P_4S_2$: C, 36.91 (37.14); H, 2.07 (2.06); S, 4.38 (5.58).

Preparation of $Fe_3(CO)_9(\mu_3\text{-}PCH_2CH_2CN)(\mu_3\text{-}PH)$ (18a) and $Fe_3(CO)_9(\mu_3\text{-}PCH_2CH_2CN)_2$ (18b). Cluster **18a** is observed by ^{31}P NMR as part of a reaction mixture including **3** and **18b** when a single equivalent of acrylonitrile (1.425 mL of a 10% THF solution of acrylonitrile, 0.217 mmol) is reacted with $Fe_3(CO)_9(\mu_3\text{-}PH)_2$ (0.01047 g, 0.0217 mmol) in 10 mL of THF. Cluster **18b** is prepared by reaction of $Fe_3(CO)_9(\mu_3\text{-}PH)_2$ (0.0076 g, 0.0157 mmol) with 3 μL (0.0456 mmol) of acrylonitrile in 6 mL of THF. After the solution stirred for 30 min, the solution color changed from red to a lighter orange-yellow. A ^{31}P NMR spectrum of the reaction mixture showed a singlet, corresponding to the desired product. Red cubic crystals of **18b** were isolated from CH_2Cl_2/hexanes (0.00471 g, 51% yield). ^1H (δ, $CDCl_3$) 3.03 (m, μ_3-PC*H*$_2$CH$_2$CN), 2.79 (m, μ_3-PCH$_2$C*H*$_2$CN). Anal. Calcd (found) for $C_{15}H_8Fe_3N_2O_9P_2$: C, 30.55 (30.46); H, 1.37 (1.30); N, 4.75 (4.66).

Preparation of $Fe_3(CO)_9(\mu_3\text{-}PCH_2CH_2CO_2Me)(\mu_3\text{-}PH)$ (19a) and $Fe_3(CO)_9(\mu_3\text{-}PCH_2CH_2CO_2Me)_2$ (19b). Clusters **19a** and **19b** were prepared analogously to **18a** and **18b**. Methyl acrylate (10 μL, 0.111 mmol) was added to a THF solution of $Fe_3(CO)_9(\mu_3\text{-}PH)_2$ (0.01186 g, 0.0245 mmol). The insertion of methyl acrylate proceeds much slower than that of acrylonitrile and required 12 h to convert completely to the double insertion product **19b**. The single insertion product, **19a**, is observed as an intermediate in the reaction. Cluster **19b** was eluted from a silica gel column in 2:1 CH_2Cl_2:hexanes and crystallized from concentrated hexanes solution (red crystals, 0.00735 g, 46%). ^1H (δ, $CDCl_3$) 3.08 (m, μ_3-PC*H*$_2$CH$_2$CO$_2$CH$_3$), 2.80 (m, μ_3-PCH$_2$C*H*$_2$CO$_2$CH$_3$), 3.75 (s, μ_3-P(CH$_2$)$_2$CO$_2$C*H*$_3$). Anal. Calcd (found) for $C_{17}H_{14}Fe_3O_{13}P_2$: C, 31.14 (31.30); H, 2.15 (2.18).

X-ray Structure Determination of $Fe_3(CO)_9(\mu_3\text{-}PH)_2$ (3). Crystallographic data and experimental parameters are summarized in Table 3. The diffraction experiment for **3** was carried out on a Rigaku AFC6S diffractometer equipped with graphite monochromated Kα radiation. Crystals suitable for analysis by X-ray diffraction were obtained by recrystallization of **3** from hexanes. Solution and refinement was performed using software from the NRCVAX computing package.[40] Least-squares refinement on F minimized the function $\sum w(|F_o| - |F_c|)^2$. Lattice parameters were determined by least-squares refinement of the setting angles of 25 high-angle reflections ($2\theta = 30°-40°$). The data collection was monitored by measurement of the intensities of three control reflections, which showed no significant intensity variation over the course of data collection. An empirical absorption correction was applied to the raw data using the intensity profiles from ψ scan data (range of transmission factors 0.44−0.66). All non-hydrogen atoms were refined using anisotropic thermal parameters. The phosphorus-bound hydrogen atoms were located in the final difference map and placed in fixed positions.

X-ray Structure Determinations for $Fe_3(CO)_9(\mu_3\text{-}PSAuPPh_3)_2$ (17) and $Fe_3(CO)_9(\mu_3\text{-}PCH_2CH_2CN)_2$ (18b). The diffraction experiments for **17** and **18b** were carried out on a Bruker SMART 1K CCD diffractometer equipped with graphite monochromated Kα radiation. Least-squares refinement on F minimized the function $\sum w(|F_o| - |F_c|)^2$. The frame data was converted to intensities using the Bruker routine SAINT and then corrected for absorption effects using SADABS. Direct methods were used to locate the heavy atoms, and the rest of the non-hydrogen positions were located with difference Fourier syntheses. All non-hydrogen atoms were included in the refinement with anisotropic thermal parameters; hydrogens were included in the final cycles at idealized positions using a riding model. Solution and refinement was performed using software from the NRCVAX computing package.[40]

Crystallographic data and experimental parameters are summarized in Table 3. A single crystal of **17** suitable for analysis by X-ray diffraction was obtained by recrystallization from THF/Et_2O solution. The crystal was mounted on the tip of a glass fiber by means of a minimal amount of oil and frozen in place in a stream of N_2 at −100 °C. Lattice parameters for **17** were determined by least-squares refinement of the setting angles of 8192 high-angle reflections ($2\theta = 3°-60°$). A single crystal of **18b** suitable for analysis by X-ray diffraction was obtained by recrystallization from CH_2Cl_2:hexanes solution. The crystal was mounted on the tip of a glass fiber by means of a minimal amount of oil. Lattice parameters for **18b** were determined by leas-squares refinement of the setting angles of 8192 high-angle reflections ($2\theta = 40°-50°$).

Acknowledgment. Partial financial support provided by the National Science Foundation (Inorganic, Bioinorganic and Organometallic Program), the Department of Education (GAANN) and the Petroleum Research Fund, administered by the American Chemical Society, is gratefully acknowledged. Partial funds for equipping the single crystal X-ray diffraction facility at UNC-CH were provided by the National Science Foundation.

Supporting Information Available: Complete ^{31}P NMR data for $[\mathbf{9}]^-$ and a related P−H dicluster; ^{31}P NMR data for the tricluster species resulting from oxidation of $[Fe_3(CO)_9(\mu_3\text{-}PH)(\mu_3\text{-}P)]^-$ $[\mathbf{4}]^-$; Tables of atomic coordinates and anisotropic thermal parameters for **3**, **17** and **18b** (PDF). An X-ray crystallographic file in CIF format. This material is available free of charge via the Internet at http://pubs.acs.org.

JA993811F

(40) Gabe, E. J.; Le Page, Y.; Charland, J.-P.; Lee, F. L.; White, P. S. *J. Appl. Crystallogr.* **1989**, *22*, 384−387.